Pergamon

Geochimica et Cosmochimica Acta, Vol. 68, No. 22, pp. 4705-4719, 2004

0016-7037/04 $30.00 + .00

doi:10.1016/j.gca.2004.04.026

# Activity disequilibrium of $^{230}$Th, $^{234}$U, and $^{238}$U in old stilbite: effects of young U mobility and $\alpha$-recoil

ROLF L. ROMER[1,*] and ALEXANDER ROCHOLL[1,2]

[1]GeoForschungsZentrum Potsdam, Telegrafenberg, D-14473 Potsdam, Germany
[2]Department für Geo- und Umweltwissenschaften, Theresienstrasse 41, Ludwig-Maximilians-Universität, D-80333 München, Germany

(*Received December* 16, 2003; *accepted in revised form April* 30, 2004)

**Abstract**—Stilbite from Malmberget and Svappavara is part of hydrothermal mineral assemblages occupying regionally occurring open Palaeoproterozoic fractures in northern Sweden. At these locations, stilbite is characterized by $Pb_{rad}$ excess relative to U and by activity ratios of $[^{234}U]/[^{238}U] > 1$ and $[^{230}Th]/[^{238}U] > 1$. The activity disequilibrium requires a disturbance of the U-Th systematics within the last one million years. Leaching and infiltration experiments on Malmberget stilbite demonstrate: (i) preferential leaching in the order Pb >U >Th and uptake in the order Pb > U, and (ii) isotopic fractionation of U by preferential mobilization of $^{238}$U and $^{235}$U relative to $^{234}$U. Stepwise-leaching further indicates that the bulk of U is hosted in the channel sites of stilbite. The Th-U disequilibrium systematics observed in untreated Malmberget and Svappavara stilbite can be explained by: (1) addition of U with $[^{234}U]/[^{238}U] > 1$ from a fluid, or alternatively (2) loss of U from a two-component system, consisting of a component that is "open" or accessible and a component that is "closed" or inaccessible to mobilization. U addition requires a multistage history involving multiple gain or loss of U and/or Pb. In contrast, U loss does not necessarily require multistage processes but can also be explained by preferential removal of $^{238}$U (and $^{235}$U) relative to recoiled daughter isotopes such as $^{234}$U, $^{230}$Th, and $^{206}$Pb (and $^{207}$Pb) during a single event. Such a behavior could be obtained if the recoiled daughter isotopes of channel-sited uranium are implanted into the crystal lattice and, in such a way, become less mobile than their parent isotopes. This case implies an open-system behavior for ions in the channel sites and a closed-system behavior for ions in the silicate framework of stilbite. Each $\alpha$-recoil directly or indirectly, i.e., through its recoil cascade, damages the silicate framework. Subsequent (continuous) low-temperature annealing of the damaged stilbite lattice could trap the recoiled daughter isotopes in the repaired crystal lattice or sealed-off channels. Such immobile recoiled material can, in part, represent the "closed" component of the system. This model can account for all observations regarding the Th-U-Pb systematics, including the Th-U disequilibrium systematics, the similarity in Th/U as deduced from Th-U disequilibrium and Pb isotope data, and the excess of radiogenic Pb ($^{208}$Pb-parents also had been multiply recoiled). These two contrasting explanations involve either multistage or multicomponent systems. They do not permit the derivation of an accurate age. 

## 1. INTRODUCTION

Stilbite ($Na_2Ca_4[Al_{10}Si_{26}O_{72}]\cdot 34H_2O$) is a zeolite mineral that commonly crystallizes in low-temperature assemblages found in open spaces such as fractures and amygdules. Due to its open crystal-structure, stilbite readily exchanges ions hosted in its three-dimensional network of channels (e.g., Szostack, 1992). Therefore, one would not expect stilbite to be a geochronologically suitable mineral at first hand. Nonetheless, Koul et al. (1981) attempted to date stilbite from the Faerøe Islands using fission-tracks and Romer (1996) demonstrated that this mineral can provide reliable $^{207}$Pb/$^{206}$Pb and U-Pb discordia-intercept ages. For stilbite from the Palaeoproterozoic Malmberget iron ore of northern Sweden, Romer (1996) obtained $^{207}$Pb/$^{206}$Pb ages that closely agree with ages of associated monazite, titanite, and apatite. Thus, stilbite appears to be capable of remaining a closed system as long as its low thermal stability (<150°C; Liou et al., 1991; Chipera and Apps, 2001) is not surpassed and as long as the mineral has not been exposed to a fluid. Such a fluid may modify the hydration of U, Th, and Pb ions according to its composition, ion charge, pH, and redox state (e.g., Breck, 1973; Townsend, 1991) and thereby mobilize these geochronologically relevant elements. The stilbite investigated by Romer (1996) almost invariably experienced significant U-loss relative to Pb. Because of the excellent agreement between the ages obtained for stilbite and associated monazite, titanite, and apatite, it was concluded that the U-loss must have occurred during the last few tens of million years. Theoretically, U-loss could have been caused: (a) by the interaction with acidic mine water in conjunction with mining over the past 300 yr, and (b) by surface fluids forced into open fractures during past glaciations. The last of these ended some 8000 yr ago and had covered the area with an ice sheet probably as thick as 3000 m (Denton and Hughes, 1981).

We have dated stilbite and titanite from the Gruvberget locality, a major iron ore deposit near Svappavara in northern Sweden, by Pb-Pb and U-Pb. We also studied the Th-U isotope systematics of this stilbite and an earlier dated stilbite from the Malmberget iron ore (sample M5 from Romer (1996)). The initial intention of the study was to use "old" stilbite to date "young" disturbances by estimating the predisturbance Th/U ratio of the old stilbite on the basis of the U-Pb and Pb-Pb systematics. Combining this value with present $[^{230}Th]/[^{232}Th]$, $[^{234}U]/[^{232}Th]$, and $[^{238}U]/[^{232}Th]$ ratios (square brackets refer to activities), allows for deriving the age of the disturbance. This concept rests on the assumptions that: (1) U

* Author to whom correspondence should be addressed (romer@gfz-potsdam.de).

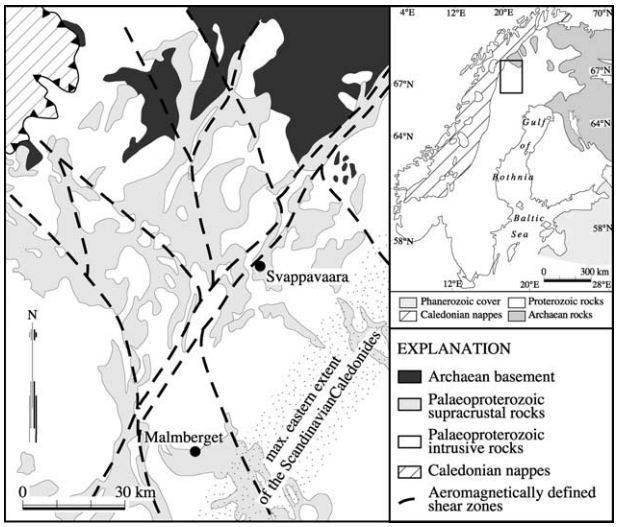


Fig. 1. Geologic sketch map of northern Sweden showing late large-scale deformation zones, the present orogenic front, and the maximum extent of the Caledonides as inferred from structural reconstructions (Romer and Bax, 1992; Romer et al., 1994) and the occurrence of radiogenic Pb in Proterozoic ore deposits of the basement (Romer and Wright, 1993). Location of the investigated stilbite veins is shown with a dot.

and its daughter products are easily mobilized from the channel sites of stilbite, and (2) the initial state of the Th-U system can be estimated from the Pb isotope systematics. Disequilibrium among U-daughters has been used in a similar way by (1) Bernat and Goldberg (1969) using the $[^{230}Th]/[^{232}Th]$ ratio of phillipsite to estimate sedimentation rates of deep sea sediments, (2) Sturchio et al. (1989) using the $^{226}Ra$-$^{230}Th$-disequilibrium to estimate the minimum duration of Ra redistribution between zeolite and water in an active hydrothermal field, and (3) Gerdes et al. (1999) to demonstrate a young disturbance of the $^{238}U$-$^{230}Th$ system in calcite from open fractures.

We present $^{238}U$-$^{234}U$-$^{230}Th$ data of Proterozoic stilbite from Malmberget and Svappavara. Stilbite from both localities shows a $[^{234}U]$ excess. In addition, Svappavara stilbite has an excess for $[^{230}Th]$. We argue that $\alpha$-recoil can explain the observed systematics due to its capability to uncouple daughter (including all isotopes from a decay chain) from parent isotopes. Implantation of the daughter isotopes into a mineralogically or crystallographically different matrix through $\alpha$-recoil may affect the specific mobilization behavior of mother and daughter isotopes during subsequent leaching or alteration.

## 2. GEOLOGIC SETTING AND INVESTIGATED SAMPLES

Iron ores in the Svappavara and Malmberget areas are hosted in a ca 1890 to 1970 my old metamorphosed volcano-sedimentary succession (e.g., Frietsch et al., 1997 and references therein). These rocks have been intruded by several generations of voluminous granites, the youngest of which have been dated at ca 1790 my (e.g., Skiöld, 1988; Romer et al., 1994; Fig. 1). At Malmberget and Svappavara, the emplacement of these late granites resulted in high-temperature low-pressure metamorphism that transformed the ore-hosting volcanic rocks into sillimanite-bearing gneisses and locally resulted in migmatization. The iron ores at Malmberget include magnetite-apatite and minor hematite-apatite bodies, whereas at Gruvberget (Svappavara) hematite-dominated assemblages are more important than magnetite-dominated assemblages. Furthermore, there are numerous NE-SW striking mafic dikes that cut the ore body.

NW-SE and NE-SE striking shear zones, generally in metasedimentary and metavolcanic rocks (Fig. 1), represent the dominant structural element in northern Sweden. They have a complex history of multiple reactivation under ductile and brittle conditions (e.g., Romer and Wright, 1993; Romer, 1996). Local stilbite-bearing fractures formed dominantly along contacts of the magnetite ore and its host-rock, due to the rheologic contrast between both units, in conjunction with movements along regional deformation zones. In the Malmberget area, stilbite-bearing fractures contain several types of hydrothermal mineral-assemblages that include variable combinations of augite, hornblende, biotite, K-feldspar, apatite, stilbite, and calcite (e.g., Flink, 1924; Romer, 1996). In contrast, fractures at Svappavara have a simpler mineral assemblage that includes titanite, stilbite, and rare calcite. At both locations, the millimeter to meter wide fractures generally remained open after being coated by stilbite, which had grown into voids and generally was not overgrown or cemented by later phases.

We investigated two stilbite-bearing hand specimens. The hand specimen from Svappavara originates from an open fracture in hydrothermally altered granitoid wallrock exposed in the open pit of the Gruvberget mine. Between the continuous stilbite coating and the wallrock, there occur locally 7 to 20 mm long, 2 to 5 mm thick, dark-brown titanite crystals that contain abundant inclusions of small magnetite crystals. Titanite is overgrown by stilbite, shows abundant fractures, and is locally altered. The stilbite "carpet" consists of 2 to 4 mm large, colorless and generally clear crystals that locally are overgrown with tiny magnetite/hematite, pyrite, and secondary Fe-hydroxides. There are also rare calcite crystals within or overgrown by the stilbite layer. The hand specimen from Malmberget has been described earlier in detail (sample M5 of the Baron Shaft; Romer, 1996). It consists of highly fractured and hydrothermally corroded K-feldspar that is intergrown with calcite and overgrown by an apatite-crust with minor magnetite and a stilbite-crust. The age of stilbite is constrained by a $^{207}Pb/^{206}Pb$ age of $1730 \pm 1$ Ma ($2\sigma$) on calcite ($^{206}Pb/^{204}Pb > 4000$) overgrown on stilbite and $^{207}Pb/^{206}Pb$ ages of 1714 to 1738 Ma on subconcordant monazite intergrown with apatite from other specimens from similar stilbite-bearing fracture coatings (Romer, 1996). In this study, stilbite, K-feldspar, and calcite from this earlier investigated stilbite specimen were used.

Backscatter electron images (Fig. 2) of Malmberget stilbite reveal mineral inclusions that are generally $<10$ $\mu$m, but in some cases may reach 200 $\mu$m in size. Although these inclusions predominantly consist of quartz and K-feldspar, some of them are phosphates and could represent important reservoirs for U, Th, and Pb. Stilbite from Svappavara shows locally a dust of dark Fe-phosphates that could be strengite. Strengite has been found in the Svappavara area as 2 to 5 mm large spherulitic structures that are built from radially arranged acicular crystals that have grown on fracture surfaces (A. Österlöf, personal communication). Since these crystals are dark and only occur on the surface of the stilbite "carpet," stilbite con-

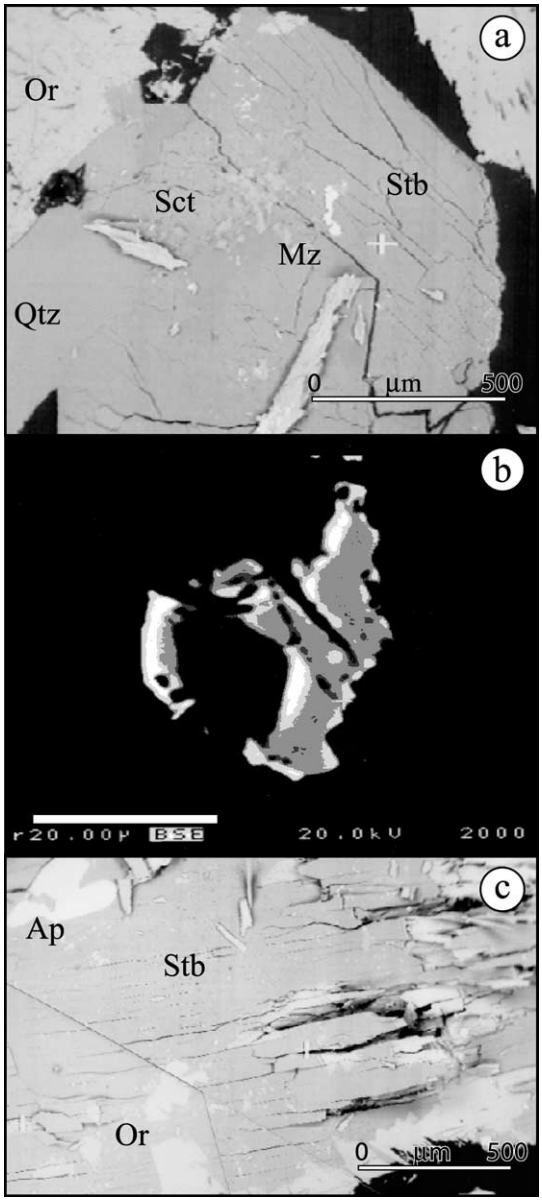


Fig. 2. Th-U-bearing inclusions in M5 Stilbite: (a) monazite inclusion, (b) close-up of the same inclusion reveals its irregular shape and segmented nature, (c) idiomorphic apatite inclusion.

centrates could be separated essentially free of this kind of contamination. In contrast, phosphate inclusions in stilbite from Malmberget include apatite and monazite (Fig. 2). These small inclusions can not be entirely avoided. Thus, the U-Th-Pb systematics of stilbite from this hand specimen may represent a mixture of two components of contrasting U, Th, and (radiogenic) Pb abundance, as well as reflecting different mobility of these elements when brought into contact with fluids.

## 3. ANALYTICAL METHODS

Titanite concentrates were washed in 7N $HNO_3$, distilled water, and acetone before dissolution. Stilbite concentrates were not acid washed before dissolution. A mixed $^{205}Pb$-$^{235}U$ isotopic tracer was added before sample dissolution. All titanite and stilbite mineral fractions were dissolved overnight in 52% HF in Savillex screw-top vials on the hot plate (160°C). HF was evaporated at 120°C and the samples were redissolved in 6N HCl. The HCl-solutions were dried at 120°C and redissolved in 3N HCl before ion-exchange chromatography on AG1-X8 using standard HCl-HBr and $HNO_3$-HCl procedures (e.g., Tilton, 1973; Manhès et al., 1978). During the measurement period total blanks were less than 15 pg for lead and less than 1 pg for uranium. All samples were analyzed on a Finnigan MAT262 multicollector mass-spectrometer at GeoForschungsZentrum Potsdam using Faraday collectors and ion counting.

For Th-U disequilibrium studies, we used the same gram-sized hand specimens of Malmberget and Svappavara as for the U-Pb work. Crystal were broken from the hand specimen and crushed to pieces $<$0.5 mm. Stilbite, alkali-feldspar, and calcite separates were handpicked under the binocular under dry conditions (the exception is fraction D10 that was picked under ethanol). The separates were then shortly rinsed in ethanol to remove stilbite powder sticking to the surface. Between 50 and 260 mg of stilbite separates were spiked with $^{229}Th$-$^{233}U$-$^{236}U$ tracers, dissolved in a Teflon beaker in HF $\pm$ $HNO_3$ and evaporated to dryness. Special care was taken to completely redissolving secondary fluorides by aqua regia treatment at c. 100°C. The separation of U and Th was similar to Chen et al. (1986) and Edwards et al. (1986). Total blanks of Th and U amounted to $\sim$15 and 10 pg, respectively. U and Th measurements were performed on a Finnigan MAT 262 thermal ionization mass spectrometer equipped with an ion counter combined with a RPQ energy filter at GeoForschungsZentrum Potsdam. U and Th separated from one sample were loaded together on the same rhenium single filament (graphite technique) and measured sequentially as metal ions. Before loading, the filaments were checked in the mass spectrometer for residual $^{232}Th$. Before each analytical session, the linearity of the ion counter system was checked and the Faraday-ion counter gain was determined using NIST (NBS) U500.

Uranium was measured using dynamic multicollection with $^{233}U$, $^{234}U$, and $^{236}U$ on the ion counter and $^{235}U$ and $^{238}U$ simultaneously on Faraday cups (in cases of low amounts of U loaded, $^{235}U$ was also detected on the ion counter). Measured isotope ratios were corrected for mass discrimination by means of the $^{233}U$-$^{236}U$ spike and were typically between 1 and 3 per mil per mass unit. Typical running temperatures ranged from 1660 to 1800°C. Depending on the signal intensity of $^{232}Th$ and the isotopic ratio, Th was measured either with $^{229}Th$ and $^{230}Th$ detected on the ion counter and $^{232}Th$ on the Faraday cup (high intensities and high $^{232}Th/^{230}Th$ ratios) or with all three isotopes measured with the ion counter. Typical $^{230}Th$ intensities were 30 to 100 cps for the low Th Svappavara samples. Running temperatures varied from 1820 to 1890°C.

Element concentrations and isotopic composition of the used mixed isotopic tracer ($^{233}U$, $^{236}U$, $^{229}Th$) were established by calibration against gravimetric Th and U standard solutions. The established composition was then checked against equilibrium standard HU-1. The U-Th concentrations and isotopic compositions were within analytical uncertainty, identical to the reference values, i.e., the measured [$^{238}U/^{230}Th$] and [$^{234}U/^{230}Th$] deviated -0.5 and 0.6% from equilibrium.

## 4. RESULTS OF LEACHING AND INFILTRATION EXPERIMENTS ON STILBITE

### 4.1. Background

In zeolite minerals, large ions as well as highly charged ions are predominantly hosted in the open channels and cavities rather than in the Si-O-framework (e.g., Flanigan and Mumpton, 1981). Whether hydrated ions in channel and cavity sites are available for ion-exchange depends mainly on the composition and ion charge of the fluid (e.g., Breck, 1973) and on the effective size of the ion (e.g., Breck, 1973; Townsend, 1991). Thus, mobility of U, Th, and Pb in stilbite may be influenced by: (1) the availability of a fluid; (2) the redox state ($U^{6+}$ is significantly more mobile than $U^{4+}$); (3) the kind and abundance of other exchangeable ions, as their absorption or struc-

tural exchange will also influence the absorption capacity of zeolite for U, Th, and Pb; and (4) the speciation of the exchangeable ions in the fluid. Published exchange experiments demonstrate that absorption and exchange selectivity of stilbite vary systematically according to $Cs^+ > Rb^+ > K^+ > Na^+ > Li^+$, and should vary similarly $Ba^{2+} > Sr^{2+} > Ca^{2+} > Mg^{2+}$ (Breck, 1973). The similar ionic radii of $Pb^{2+}$ and $Ca^{2+}$ (and $Sr^{2+}$) suggests that Pb may behave similarly to Ca and Sr and thus be rather strongly adsorbed onto stilbite. Such exchange should especially affect the outer parts of zeolite crystals, where channel sites are less likely to be blocked by large hydrated ions.

### 4.2. Leaching Experiments

Three batches of stilbite (Zeo-5, Zeo-6, Zeo-114) were stepwise leached, starting with water and followed by increasingly stronger acids (Table 1). The experiment demonstrates significant mobility of Pb, U, and, to a lesser extent, Th, in the zeolite. Most importantly, it establishes the relative mobilities of these elements in a zeolite-fluid system. Laboratory conditions differ from natural leaching conditions in several respects: (1) The U-Pb systematics of Malmberget stilbite (Romer, 1996) indicates that the starting material had already lost some 90% U relative to Pb; (2) The water and acids used for the leaching experiment were multiply distilled, possibly allowing release of more channel-hosted ions during the experiment than under natural conditions; (3) The amount of material leached depends on the fluid-zeolite ratio; (4) The experimental setup excludes possible gains of U, Th, and Pb from the fluid (see below); and (5) The acids used were much stronger than in natural fluids. Although the experimental setup does not allow strict application to natural systems, the results give some important clues regarding the relative mobility of Pb, U, and Th in a zeolite-fluid system. The experiment demonstrates significant mobility of Pb, U, and, to a lesser extent, Th between zeolite and an aqueous fluid.

Although stilbite Zeo-114 (Malmberget) has distinctly higher U and Pb contents than the stilbite batches Zeo-5 and Zeo-6 (Svappavara; Table 1) and not all stilbite batches were leached applying the same procedure, acid types, and acid strength, all Svappavara stilbite batches show a similar leaching behavior. All leaching experiments demonstrate that the bulk of Pb and U is readily leachable by water and diluted HCl, indicating that these elements are hosted in the channel sites. For instance, the residues of stilbite concentrates Zeo-5 and Zeo-6 contain only ~1% of the total Pb and only 2 to 5% of the total U. Taking into consideration that the starting material probably had already lost ~ 90% of its U, less than 0.5% of the predisturbance U might have been hosted in the silicate-lattice. The leaching experiments furthermore indicate that Pb and U have been mobilized to different degrees and are, therefore, strongly fractionated from each other. For example, U is preferentially lost during exposure to $H_2O_{dist}$ and weak acids, whereas Pb is dominantly lost during the leaching steps with stronger acids.

### 4.3. Infiltration Experiments

We used a stilbite batch (Zeo-115) from the Malmberget specimen to investigate the infiltration capability of its channel sites with respect to U, Th, and Pb. For this purpose, 0.1 to 1.0 mm large fragments of stilbite were brought into contact for 19 h at 70°C with a slightly alkaline tracer solution of $H_2O$ (pH adjusted to 8.5 by addition of $NH_4OH$) doped with 66 pmol $^{235}U$, 13 pmol $^{229}Th$, and 0.38 pmol $^{205}Pb$ tracers. Thereafter, crystals and solution were separated from each other and the crystals were briefly rinsed with water that was recombined with the tracer solution (Table 2). The results indicate that U, Th, and Pb were lost from the channel sites into the solution, in agreement with the results from the leaching experiment. An additional and opposite transport direction, i.e., from solution to channel sites, is demonstrated by the significantly lowered $^{238}U/^{235}U$ ratio and the presence of $^{229}Th$ and $^{205}Pb$ in the solid fraction. These observations indicate a mutual exchange of U, Th, and Pb between crystal and solution, in addition to a net loss of U, Th, and Pb from the crystal. Assuming the original concentrations of U, Th, and Pb in this stilbite sample were similar to those of stilbite Zeo-114 (which is an aliquot from the same batch of crystal fragments; Table 1), the isotopic composition of the solution and the crystals can be used to mass-balance the amount of tracer elements that infiltrated into the stilbite channels and the amount of channel-derived elements lost to the solution (Table 2). The contrasting distribution of Pb, U, and Th between fluid and residue is controlled by the solubility of the element, charge and size of the hydrated ions, and their adsorption coefficient. We suggest the following interpretation regarding the distribution of tracer between solution and residue (Table 2): (1) Little tracer-U is incorporated into the crystal as the large hydration envelope of the highly charged $U^{6+}$-ion hinders incorporation into channel sites; (2) Tracer-Pb is readily incorporated into the channel sites as it is less charged, and therefore has a smaller hydration envelope than U; and (3) Tracer-Th appears to be most easily lost from solution. Because Th is only slightly soluble in aqueous solutions and because Th should not fit fundamentally more easily into the channel sites than U, we interpret the apparent enrichment of tracer-Th in the crystalline fraction to adsorption on stilbite or the reaction vial. If Th is lost to adsoption on the vial walls, the total amount of Th adsorption on the surface of stilbite is overestimated as is the $K_D$ between solid and fluid. Fractionation of element pairs during leaching (apparent $K_D$ values in Table 2) suggests an order of mobility according to Pb >U >Th.

The redistribution of Th, U, and Pb between solid and fluid phase is a continuous process that is controlled by the abundance of these elements in the solid and fluid phases, the ratio of fluid to solid phase, and by element-specific distribution coefficients that, in turn, are a function of solubility, temperature, and fluid composition (pH, ionic strength, complexing ligands, etc.). For a fluid-mineral system in open fractures, such as the investigated Svappavara and Malmberget locations, two extreme scenarios can be envisaged: (i) The fracture is "dry." The minerals may be coated by a fluid film. This film, however, is not exchanged with time and, thus, represents a "stationary" fluid; (ii) The fracture is percolated by a fluid and the mineral is in contact with continuously exchanging volumes of the fluid. For a "stationary" fluid: (1) equilibrium is reached between fluid and solid, and (2) combined fluid and solid represent a closed system. Subsequent redistribution of these elements between stilbite and fluid involves essentially the same

Table 1. U-Pb analytical results for stilbite experiments.[e]

| Sample[a] | | Pb (ppb) | U (ppb) | Th (ppb) | $^{204}Pb$[b] (pmol) | $^{206}Pb$[b] (pmol) | $^{207}Pb$[b] (pmol) | $^{208}Pb$[b] (pmol) | $^{238}U$[c] (pmol) | Th[d] (pmol) | $^{206}Pb/^{204}Pb$[e] | $^{207}Pb/^{204}Pb$[e] | $^{208}Pb/^{204}Pb$[e] | Fu[f] | $F_{Th}$[f] | $[^{234}U]/[^{238}U]$ |
|---|---|---|---|---|---|---|---|---|---|---|---|---|---|---|---|---|
| **Zeo-5** (Svappavara) sample size: 137.45 mg | | | | | | | | | | | | | | | | |
| 13 | $H_2O$-wash | 34.0 | 5.0 | — | 0.277 | 5.81 | 4.44 | (12.0) | 2.87 | — | 21.96 | 16.04 | — | 1.8 | | |
| 14 | 0.4N HCl | 124 | 6.2 | — | 0.930 | 23.9 | 15.3 | 42.1 | 3.54 | — | 25.74 | 16.47 | 45.26 | 0.2 | | |
| 15 | Aqua Regia | 17.9 | 3.7 | — | 0.105 | 4.07 | 1.90 | 5.81 | 2.12 | — | 38.64 | 17.99 | 55.12 | 0.6 | | |
| 16 | Residue | 0.6 | 0.3 | — | 0.005 | 0.114 | 0.079 | 0.208 | 0.170 | — | 23.35 | 16.12 | 42.56 | | | |
| | **Sum**[g] | 177 | 15.2 | | 1.32 | 33.9 | 21.7 | (60.0) | 8.70 | | 25.8 | 16.5 | (45.6) | | | |
| **Zeo-6** (Svappavara) sample size: 53.92 mg | | | | | | | | | | | | | | | | |
| 17 | $H_2O$-wash | 24.4 | 7.7 | — | 0.074 | 1.83 | 1.20 | 3.25 | 1.73 | — | 24.91 | 16.32 | 44.11 | 4.9 | | |
| 18 | 0.4N HCl | 39.8 | 3.5 | — | 0.125 | 2.84 | 2.02 | 5.38 | 0.785 | — | 22.74 | 16.14 | 43.04 | 1.6 | | |
| 19 | 3.1N HCl | 85.7 | 3.9 | — | 0.232 | 6.91 | 3.94 | 11.2 | 0.884 | — | 29.74 | 16.95 | 48.35 | 0.3 | | |
| 20 | Residue | 1.8 | 0.3 | — | 0.006 | 0.136 | 0.090 | 0.233 | 0.070 | — | 24.1 | 15.9 | 41.3 | | | |
| | **Sum**[g] | 152 | 15.4 | | 0.437 | 11.7 | 7.24 | 20.1 | 3.46 | | 26.85 | 16.6 | 46.03 | | | |
| **Zeo-114** (Malmberget) sample size: 88.85 mg | | | | | | | | | | | | | | | | |
| 21 | $H_2O + NH_4OH$ (pH = 8.5) | 69.3 | 1182 | — | 0.204 | 16.4 | 4.520 | 8.681 | 437.95 | — | 80.55 | 22.21 | 42.65 | 18.3 | | |
| 22 | $H_2O$ (pH = 7) | 14.1 | 72.8 | 0.295 | 0.049 | 2.98 | 0.989 | 2.02 | 27.0 | 0.113 | 60.68 | 20.14 | 41.17 | 4.7 | 4.0 | 1.91 ± 0.03[h] |
| 23 | 1N HCl | 4400 | 4050 | 16.22 | 10.6 | 1140 | 262 | 476 | 1500 | 6.21 | 107.5 | 24.67 | 44.83 | 8.3 | 1.1 | 1.47 ± 0.02[h] |
| 24 | 2.5N $HNO_3$ | 699 | 63.2 | 0.592 | 1.71 | 181 | 41.1 | 76.6 | 23.4 | 0.227 | 106.1 | 24.09 | 44.91 | 0.6 | 0.1 | 1.85 ± 0.05[h] |
| 25 | Residue | 428 | 61.8 | 3.3 | 1.03 | 112 | 24.9 | 46.4 | 22.9 | 1.31 | 108.5 | 24.25 | 45.09 | | | 2.55 ± 0.04[h] |
| | **Sum**[g] | 5610 | 5430 | (20.4) | 13.6 | 1450 | 334 | 610 | 2010 | (7.86) | 106.8 | 24.51 | 44.82 | | | |

[a] Zeolite samples were separated under the binocular. Zeolite samples were never immersed in any fluid during purification. For the leaching experiment, samples were stored in each solution for 24h. The beakers were repeatedly agitated in an ultrasonic bath. Solutions were centrifuged and decanted. The solid residue was rinsed with distilled water, agitated in the ultrasonic bath. The wash solution was after renewed centrifugation decanted and combined with the first solution. 0.4N and 3.1 N HCl leach solutions and residue solutions of zeolite 5 were split by weight before tracer addition. One part was spiked with $^{229}Th$ and $^{233}U$–$^{236}U$ tracer solutions. The other part and all solutions from sample Zeo-6 were spiked with a mixed $^{205}Pb$–$^{235}U$ tracer. The $H_2O$-wash of sample Zeo-5 was spiked with a mixed $^{208}Pb$–$^{235}U$ tracer. Reported contents of individual isotopes in pmol have been adjusted to refer to the total sample, rather than the individual spiked splits. Content and concentration data refer to the amount of U, Pb, and Th mobilized from the crystal by respective solution.

[b] Corrected for 10 pg Pb-blank.

[c] Corrected for 0.5 pg U-blank.

[d] Corrected for 0.5 pg Th-blank.

[e] Analyzed on a Finnigan MAT262 multicollector mass spectrometer in static mode using Faraday collectors and secondary electron-multipliers in ion-counting mode. Data corrected for 0.1% per atomic mass unit. mass discrimination, tracer contribution, and 10 pg lead blank. Analytical uncertainties are less than 0.2–0.3% except for residue samples, where the sample size is small in comparison to the amount of blank lead. These ratios are not better known than 0.5% to 1%. For all samples, the blank contribution poses the major source of uncertainty.

[f] Enrichment factor reflecting the preferential loss of U or Th to the solution (for values >1) and the preferentiall loss of Pb (for values <1). $F_u$ is defined as $(^{238}U/^{204}Pb)_{solution}/(^{238}U/^{204}Pb)_{residue}$. Similarly for $F_{Th}$. Note that the zeolite bulk samples already had lost U, as their $^{206}Pb/^{238}U$ is too high in relation to their $^{206}Pb/^{204}Pb$ and the age of the samples, as given by the U-Pb titanite age (cf. Table 1 and Fig. 4). Earlier U-loss relative to Pb amounted to ca 90% for Zeo-5, 90% for Zeo-6, and 60% for Zeo-114.

[g] Calculated by addition of the contents of the three leachates and the residue for each zeolite sample. The lead isotopic composition represents the weighted mean. Expressions in parantheses refer to values derived from incomplete analyses, whereby the contribution of the lacking fraction is considered to be minor. No values are given if the lacking fraction could be expected to give a significant contribution to the total.

[h] Uncertainties in $2\sigma_m$.

Table 2. U-Pb analytical results for stilbite infiltration experiment.

| Sample[a] | Pb[b] (pmol) | U[b] (pmol) | Th[b] (pmol) | % Pb[d] Tracer | % U[d] Tracer | % Th[d] Tracer | % Pb[e] Sample | % U[e] Sample | % Th[e] Sample | U/Th | Pb/U | Pb/Th |
|---|---|---|---|---|---|---|---|---|---|---|---|---|
| **Zeo-115** (Malmberget) sample size: 18.05 mg | | | | | | | | | | | | |
| Solution[c] | 62.41 | 11.48 | 0.138 | 88 | >99 | 15 | 43 | 10 | 1 | 83.2 | 5.44 | 452 |
| Residue[c] | 83.43 | 106.9 | 8.94 | 12 | <0.07 | 85 | 57 | 90 | 99 | 11.96 | 0.78 | 9.33 |
| $K_D$[f] | | | | | | | | | | ~7[f] | ~7[f] | ~48[f] |

[a] Zeolite samples were separated under the binocular microscope. Zeolite fragments were stored in an aqueous solution (pH adjusted to 8.5 using $NH_4OH$) with defined amounts of $^{235}U$, $^{229}Th$, and $^{208}Pb$ for 19 hr on a hot plate at 70°C.

[b] Concentration of U, Th, and Pb is assumed to be identical to sample Zeo-114, which is a split from the same mineral concentrate and was used for the leaching experiment (Table 1). Distribution of U, Th, and Pb between solid and solution is estimated for each element from the isotopic composition of solid and solution in combination with mass balance calculation. Mass balance takes into account that the tracers are redistributed between solid and solution.

[c] Distribution of tracer between solid and solution (based on mass balance calculation).

[d] Distribution of U, Th, and Pb as estimated from the isotopic composition and the amount of tracer isotope present in the solution and the residue, respectively.

[e] Fractionation of U, Th, and Pb between fluid and solid. All ratios are atom ratios.

[f] $K_D$ for element pairs between fluid and solid. Defined as $K_D = (U/Th)_{fluid}/(U/Th)_{solid}$. Analogue for other ratios. Calculations takes contributions from the isotopic tracer into consideration.

material, which in turn makes stilbite a pseudoclosed system, especially if the bulk amount of Th, U, and Pb is contained in stilbite. In contrast, for the case of a percolating fluid (open system), stilbite exchanges with continuously different volumes of fluid. No equilibrium can be reached, because elements lost from stilbite to the fluid are transported away and elements gained by stilbite have no relation to the earlier history of stilbite. For instance, if the Pb content in the fluid is too low to be in equilibrium with the mineral, Pb is lost from stilbite until equilibrium is reached. If the Pb content in the fluid is too high to be in equilibrium, stilbite will incorporate Pb derived from the fluid. The same principle applies to U and Th. Thus, depending on the relative concentration of U, Th, and Pb in the fluid and the mineral, each element is mobilized independently and to a specific extent as a function of its distribution coefficient. Continuous percolation of a fluid may eventually result in a scenario where the isotopic composition of the fluid and stilbite are identical, and the concentration Pb, U, and Th in stilbite is in equilibrium with the contents of these elements in the fluid. In this special case, exchange between stilbite and fluid results in a Pb-U-Th systematics indistinguishable from the pseudoclosed system obtained for a "stationary" fluid.

## 5. U-Pb AGES AND Pb-Pb SYSTEMATICS OF TITANITE, STILBITE, AND LEACHATES

Six titanite mineral fractions, representing fragments of a single 20 mm large titanite crystal, yield concordant U-Pb data (Fig. 3). The $^{207}Pb/^{206}Pb$ ages span a range from 1765 to 1774 Ma (Table 3). This indicates that the titanite fractions had experienced a disturbance in the first few tens of million years after crystallization. The best age estimate for the crystallization of the titanite is probably given by the three fractions with the oldest $^{207}Pb/^{206}Pb$ ages, i.e., 1773.0 ± 0.7 Ma ($2\sigma$; Fig. 3). The minimum age estimate for the disturbance is given by the youngest $^{207}Pb/^{206}$ Pb age, i.e., 1764 Ma (Table 3). Even though the $^{206}Pb/^{204}Pb$-$^{208}Pb/^{204}Pb$ systematics of the fractions shows titanite scatter, the $^{232}Th/^{238}U$ atomic ratio of the fractions calculated from $^{208}Pb_{rad}/^{206}Pb_{rad}$ is rather uniform and close to 1.5 (Fig. 4a). Large titanite crystals are found only along the fracture surface, but not within the hydrothermally affected wallrock. Therefore, titanite formed during hydrothermal fluid flow within this fracture rather than during the crystallization of the host-rock. Hence, the weighted $^{207}Pb/^{206}Pb$

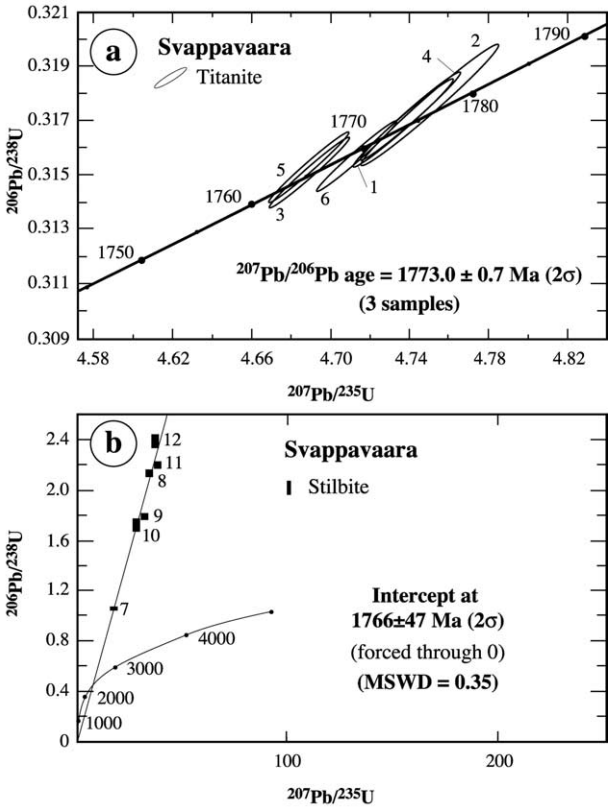


Fig. 3. Concordia diagram for titanite and stilbite from Svappavara. All diagrams plotted and calculated using ISOPLOT 2.71 (Ludwig, 1994).

Table 3. U-Pb analytical results for titanite and stilbite from a Svecofennian fracture mineralization, Svappavaara iron ore, northern Sweden.

| Sample[a] | Weight (mg) | Concentrations (ppm) U | Concentrations (ppm) Pb | $^{206}Pb/^{204}Pb$ Measured ratios[b] | $^{206}Pb/^{204}Pb$[c] | $^{207}Pb/^{204}Pb$[c] | $^{208}Pb/^{204}Pb$[c] | Atomic ratios[d] $^{206}Pb/^{238}U$ | $^{207}Pb/^{235}U$ | $^{207}Pb/^{206}Pb$ | Apparent ages (Ma)[e] $^{206}Pb/^{238}U$ | $^{207}Pb/^{235}U$ | $^{207}Pb/^{206}Pb$ |
|---|---|---|---|---|---|---|---|---|---|---|---|---|---|
| **Titanite** | | | | | | | | | | | | | |
| 1 (2) | 0.223 | 158 | 67.8 | 1813 | 1892 | 218.8 | 845.3 | .31689 | 4.7369 | 0.10841 | 1775 | 1774 | 1773 |
| 2 (2) | 0.201 | 171 | 74.8 | 1357 | 1401 | 165.7 | 650.4 | .31760 | 4.7501 | 0.10847 | 1778 | 1776 | 1774 |
| 3 (2) | 0.235 | 173 | 75.4 | 2223 | 2332 | 265.4 | 1126 | .31507 | 4.6894 | 0.10795 | 1766 | 1765 | 1765 |
| 4 (3) | 0.317 | 190 | 84.5 | 3004 | 3132 | 353.0 | 1580 | .31736 | 4.7434 | 0.10840 | 1777 | 1775 | 1773 |
| 5 (2) | 0.331 | 89.4 | 39.7 | 1666 | 1751 | 202.5 | 883.8 | .31532 | 4.6896 | 0.10787 | 1767 | 1765 | 1764 |
| 6 (2) | 0.239 | 167 | 71.0 | 2641 | 2793 | 316.1 | 1238 | .31574 | 4.7136 | 0.10827 | 1769 | 1770 | 1771 |
| **Stilbite** | | | | | | | | | | | | | |
| 7 (6) | 3.540 | 0.028 | 0.364 | 21.256 | 21.19 | 15.96 | 41.47 | 1.07 | 16 | 0.105 | — | — | 1715 |
| 8 (5) | 4.458 | 0.013 | 0.357 | 21.113 | 21.03 | 15.97 | 41.39 | 2.18 | 33 | 0.109 | — | — | 1790 |
| 9 (3) | 3.238 | 0.016 | 0.375 | 20.732 | 20.62 | 15.93 | 40.99 | 1.76 | 27 | 0.111 | — | — | 1813 |
| 10 (3) | 4.138 | 0.011 | 0.184 | 23.347 | 23.20 | 16.18 | 43.01 | 1.75 | 26 | 0.106 | — | — | 1734 |
| 11 (4) | 3.202 | 0.010 | 0.189 | 24.474 | 24.48 | 16.34 | 44.04 | 2.22 | 33 | 0.109 | — | — | 1779 |
| 12 (4) | 4.348 | 0.010 | 0.191 | 24.722 | 24.73 | 16.36 | 44.24 | 2.41 | 36 | 0.108 | — | — | 1764 |

[a] Titanite and stilbite were selected under the binocular. Only small, inclusion-free fragments from a large titanite crystal were used. Some stilbite crystals had tiny inclusions of presumably pyrite or strengite. Stilbite was separated under alcohol and was rinsed in distilled water in the ultrasonic before dissolution. Numbers in parantheses refer to the number of fragments or crystals analyzed.

[b] Lead isotope ratios corrected for 0.1% per atomic mass unit fractionation and isotopic tracer.

[c] Lead corrected for fractionation, 15 pg Pb blank, isotopic tracer

[d] Lead corrected for 0.1% per A.M.U. fractionation, blank, isotopic tracer, and initial lead ($^{206}Pb/^{204}Pb = 15.50 \pm 0.03$, $^{207}Pb/^{204}Pb = 15.36 \pm 0.03$, $^{208}Pb/^{204}Pb = 35.6 \pm 0.1$). U corrected for 0.1% per atomic mass unit fractionation and 1 pg U blank. Uncertainties of $^{206}Pb/^{238}U$, $^{207}/Pb/^{235}U$, and $^{207}Pb/^{206}Pb$, range from 0.33–0.59%, 0.36–0.62%, and 0.06–0.10%, respectively, for titanite and from 2.2–3.0%, 5.2–10.5%, and 4.4–9.3%, respectively, for stilbite. These uncertainties and the error correlation between $^{206}Pb/^{238}U$ and $^{207}Pb/^{235}U$ Of 0.98–0.99 (titanite) and 0.48–0.58 (stilbite) largely depend on the measured $^{206}Pb/^{204}Pb$. All uncertainties were calculated taking into consideration measurement errors, 30% uncertainty for the fractionation correction, 50% uncertainty for the blank level, and above uncertainties for the common Pb composition and comparable uncertinties for blank Pb composition. The uncertainty of $^{205}Pb/^{235}U$ in the tracer is less than 0.3%. Data reduction was performed by Monte Carlo modelling of 1000 random normally distributed data sets that fit above uncertainty limits, allowing for error correlation when appropriate.

[e] Apparent ages were calculated using the constants of Jaffey et al. (1971) recommended by IUGS (Steiger and Jäger,1977).

age at 1773 Ma represents the best estimate for the minimum age of the fracture. Titanite along with the fracture wall is coated with stilbite, implying that stilbite is younger. The slightly disturbed U-Pb systematics of titanite might be related to the formation of the stilbite rim. This leaves open whether stilbite and titanite crystallized during entirely different events of fluid flow from isotopically and chemically different fluids.

Six stilbite mineral separates define a linear trend within error on the $^{206}Pb/^{204}Pb$-$^{207}Pb/^{204}Pb$ diagram (MSWD = 1.03) that corresponds to an age of 1750 ± 110 Ma ($2\sigma$), if interpreted as an isochron (Fig. 4b). The large age uncertainty originates from the small range in isotopic composition (Table 3). On a concordia diagram, the same data appear highly disturbed. They plot far above the concordia (Fig. 3b), implying either U-loss or Pb-gain. Such a behavior of stilbite has been observed earlier (Romer, 1996) and was interpreted as U-loss rather than Pb-gain. The discordia intercepts the concordia at 1766 ± 47 Ma ($2\sigma$, forced through the diagram origin, MSWD = 0.346), which agrees with the U-Pb age of titanite within analytical error. As the Pb systematics appear unaffected, the disturbance of the U-Pb systematics of stilbite must have occurred during the last few tens of my. The degree of discordance of the stilbite concentrates requires a loss of 70 to 85% of U relative to Pb, which is similar to the relative U-loss reported in an earlier study (Romer, 1996). This estimate indicates initial U contents in the range of 62 to 95 ppb or higher if Pb were also lost. The time-integrated Th/U ratio and the initial Th contents can be estimated from the excellent linear alignment of the stilbite data in the $^{206}Pb/^{204}Pb$-$^{208}Pb/^{204}Pb$ diagram (Fig. 4b). The $^{232}Th/^{238}U$ atomic ratio derived in such a way is 2.68, which corresponds to estimated Th contents of 166 to 254 ppb. Note that the time-integrated $^{232}Th/^{238}U$ ratio derived from Pb-isotopes is considerably higher in stilbite (~2.7) compared to titanite (~1.5; Fig. 4a). Thus, the radiogenic Pb of stilbite can not represent Pb that was mobilized from titanite and scavenged by stilbite.

The leachates from two experiments using Svappavara stilbite fall on the same isotopic trend as untreated Svappavara bulk stilbite (Table 3). Exceptions include the $H_2O$ leachate (concentrates 13 and 17, Fig. 4c) and possibly the residues after leaching (concentrates 16 and 20, Fig. 4c). We explain the deviation of these data from the common trend as following: The $H_2O$ leachates contained significant contributions from easily mobilized Pb adsorbed on the crystal surface. This Pb probably originated from different sources and may have been multiply redistributed. The residues represent less than 1.2% of the total stilbite Pb. The Pb isotopic composition of these small samples (80 and 100 pg Pb) is not well known and overlaps within its large error with the regression line. The coincidence of bulk and leach data on the same line suggests that the Pb isotopic composition either reflects a single-stage history or a young two-component mixing event.

The Pb isotopic composition of the Malmberget stilbite leachate suggests that Pb released during the first two leaching steps originates from a different source than the later released Pb (Table 1). Early released Pb is distinctly less radiogenic than later released Pb. This probably indicates the presence of com-

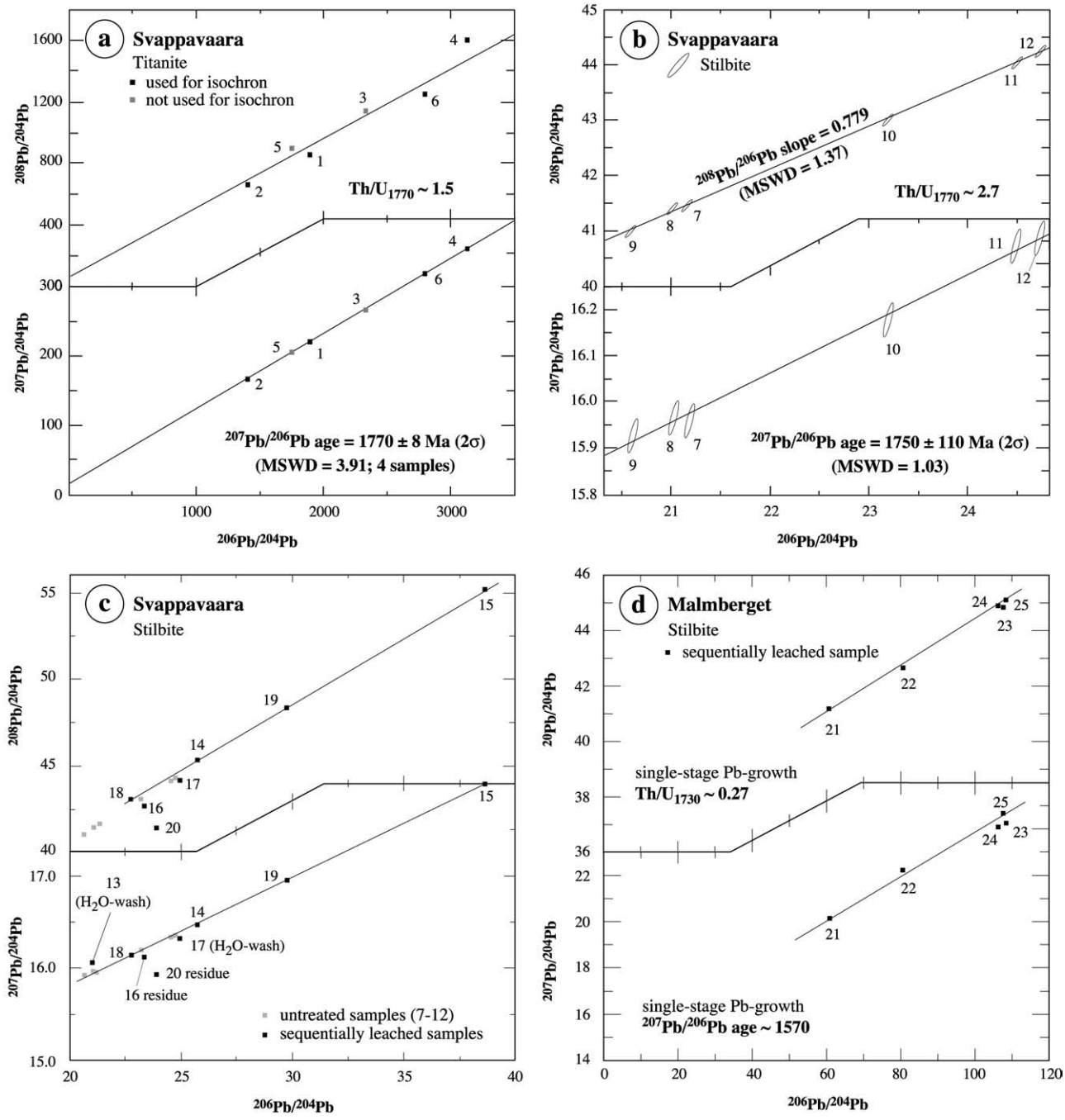


Fig. 4. Pb isotope diagrams for titanite from Svappavara and stilbite fractions from Malmberget and Svappavara. The good linear alignment in the $^{206}Pb/^{204}Pb$–$^{207}Pb/^{204}Pb$ diagrams is interpreted as an isochron in the case of titanite and as rotated mixing line for the leachates of the stilbite concentrates from Malmberget. The good linear alignment in the $^{206}Pb/^{204}Pb$–$^{208}Pb/^{204}Pb$ diagram is used to estimate the time-integrated Th/U of the various fractions. Numbers refer to Tables 1 and 3.

mon Pb that was scavenged from fluids passing over the mineral surface (or acquired through exchange of stilbite Pb with fluid Pb). Pb released by acids is distinctly more radiogenic and isotopically uniform. All leach fractions roughly define a linear trend in the Pb-isotope diagrams (Fig. 4d). The $^{207}Pb/^{206}Pb$ slope is too flat to agree with a single-stage history for zeolite starting at 1730 Ma, which is the Pb-Pb age of calcite ($^{206}Pb/^{204}Pb$ >4000) that has overgrown the stilbite (Romer, 1996).

## 6. $^{238}U$-$^{234}U$-$^{230}Th$-$^{232}Th$ SYSTEMATICS

### 6.1. $^{230}Th/^{232}Th$ vs. $^{238}U/^{232}Th$ Systematics

The Th/U systematics of >1 my old undisturbed minerals is in activity equilibrium. This implies that the atomic ratio of $^{230}Th/^{232}Th$ is directly proportional to $^{238}U/^{232}Th$ through the relations $[^{230}Th] = [^{238}U]$ and $^{230}Th_{at} = {}^{238}U_{at} \cdot \lambda_{238}/\lambda_{230}$ (e.g.,

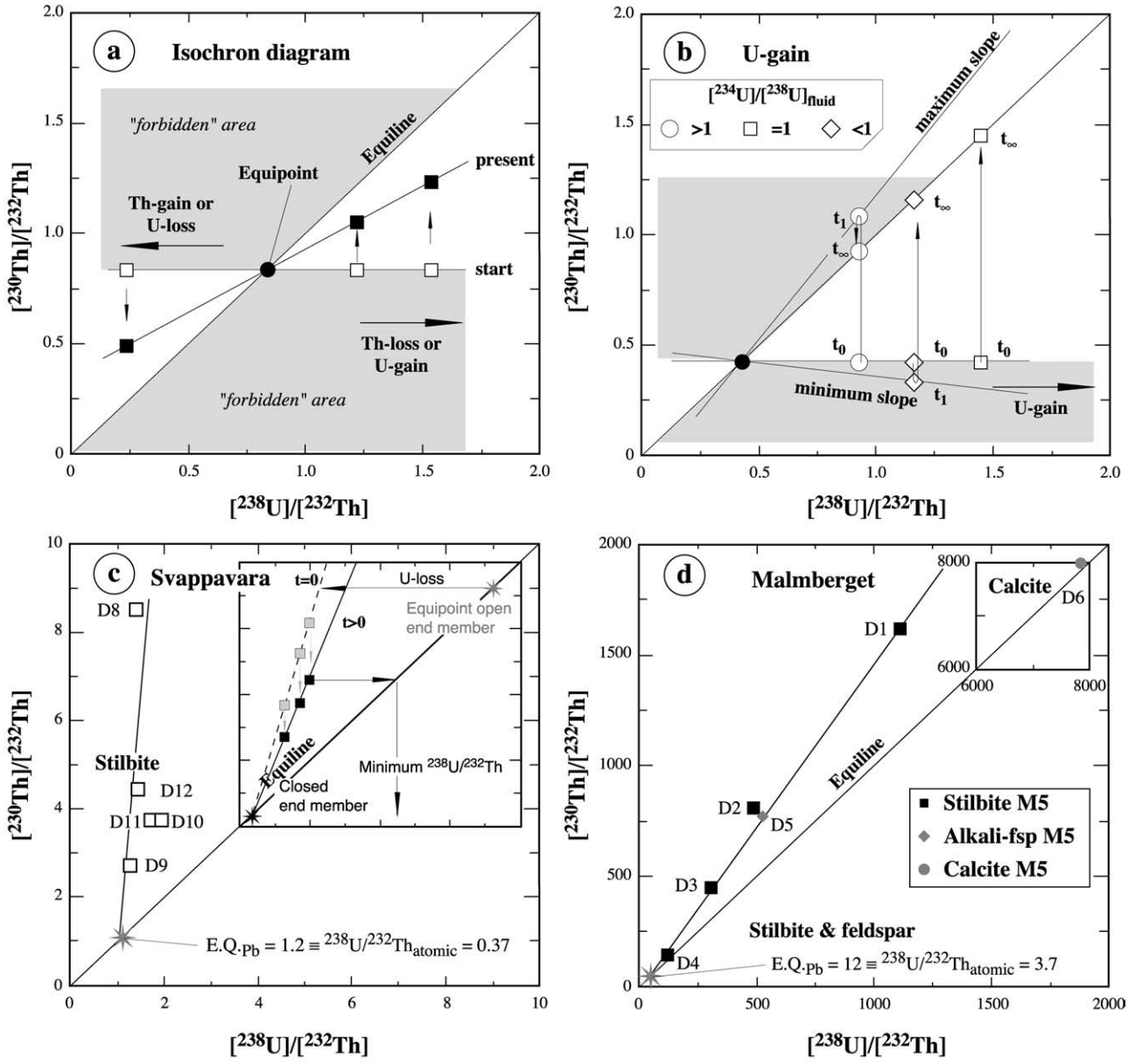


Fig. 5. [$^{230}$Th]/[$^{232}$Th]-[$^{238}$U]/[$^{232}$Th] diagram: (a) and (b) principal behavior of Th-U disequilibrium system, (c) data for stilbite from Svappavara, (d) data for stilbite, alkalifeldspar, and calcite from Malmberget. All data from Table 4. Inset in (c) shows the two-component mixing between an inert component and a component that experienced U-loss. Reference lines through stilbite data in (c) and (d) are drawn arbitarily. Asterisk corresponds to [$^{238}$U]/[$^{232}$Th] as derived from the Pb isotopes and the age of stilbite from Malmberget and Svappavara, respectively.

Faure, 1986). Samples which are in activity equilibrium fall on the equiline in the [$^{230}$Th]/[$^{232}$Th]-[$^{238}$U]/[$^{232}$Th] diagram (e.g., Allègre and Condomines, 1976; Fig. 5a). A fractionation of U from Th (without fractionation between $^{238}$U and $^{234}$U and between $^{232}$Th and $^{230}$Th) shifts the data from the equiline. The loss of U results in $^{230}$Th "excess" (Fig. 5a). With time, excess $^{230}$Th diminishes until activity equilibrium has been reached. The age of the disturbance can be calculated from an isochron, assuming that there is no fractionation beween $^{238}$U and $^{234}$U and between $^{230}$Th and $^{232}$Th.

U-gain shows the same principal features (although it will displace the data to the right side of the equiline), as long as [$^{234}$U]/[$^{238}$U]$_{mineral}$ = [$^{234}$U]/[$^{238}$U]$_{fluid}$ (Fig. 5a). This condition may rarely be fulfilled, especially for minerals in activity equilibrium. For [$^{234}$U]/[$^{238}$U]$_{mineral}$ < [$^{234}$U]/[$^{238}$U]$_{fluid}$ (open circles in Fig. 5b), there is fast initial ingrowth of $^{230}$Th due to excess $^{234}$U. This results in an overestimation of the age and eventually in an "overshooting" of the equiline. The extent of such an "overshot" depends on the [$^{234}$U]/[$^{238}$U] ratio of the fluid. After having reached a maximum, the slope of the oversteep isochron flattens with increasing time, and the isotopic values approach the equiline from the "wrong" side, i.e., from above (Fig. 5b). The slope of such an isochron will never yield a correct age estimate. The nonideal starting conditions, how-

Table 4. Concentration and activity ratios of U and Th.

| Sample[a] | | wgt (mg) | U (ppb) | Th | $^{238}U/^{232}Th$[b] atomic ± $2\sigma_m$ | $[^{234}U]/[^{238}U]$[b] $\pm 2\sigma_m$ | $[^{230}Th]/[^{234}U]$[b] $\pm 2\sigma_m$ | $[^{238}U]/[^{232}Th]$[b] $\pm 2\sigma_m$ | $[^{230}Th]/[^{232}Th]$[b] $\pm 2\sigma_m$ |
|---|---|---|---|---|---|---|---|---|---|
| **M-5** (Malmberget) | | | | | | | | | |
| D1 | Stilbite | 157.58 | 9420 | 25.9 | 354.6 ± 9.6 | 1.498 ± 0.025 | 0.981 ± 0.025 | 1110 ± 30 | 1633 ± 26 |
| D2 | Stilbite | 130.62 | 8260 | 49.7 | 157.5 ± 7.0 | 1.508 ± 0.036 | 1.06 ± 0.14 | 494 ± 22 | 790 ± 93 |
| D3 | Stilbite | 148.56 | 15420 | 156 | 95.66 ± 0.41 | 1.448 ± 0.005 | 1.046 ± 0.007 | 299.9 ± 1.3 | 454.6 ± 2.4 |
| D4 | Stilbite | 58.30 | 578 | 14.4 | 38.98 ± 0.70 | 1.238 ± 0.011 | 1.000 ± 0.073 | 122.2 ± 2.2 | 151 ± 11 |
| D5 | Alk-fsp | 47.87 | 68600 | 405 | 164.8 ± 3.5 | 1.496 ± 0.012 | 1.008 ± 0.007 | 517 ± 11 | 779.5 ± 4.9 |
| D6 | Calcite | 3.00 | 132000 | 53.2 | 2502 ± 42 | 0.984 ± 0.013 | 1.044 ± 0.024 | 7840 ± 130 | 8064 ± 160 |
| **SVAP** (Svappavaara) | | | | | | | | | |
| D7 | Stilbite | 138.39 | 13.6 | 38.3 | 0.3452 ± 0.0051 | 1.598 ± 0.050 | — | 1.082 ± 0.016 | — |
| D8 | Stilbite | 117.40 | 16.6 | 44.3 | 0.3620 ± 0.0029 | 1.422 ± 0.040 | 5.25 ± 0.23 | 1.135 ± 0.009 | 8.42 ± 0.48 |
| D9 | Stilbite | 212.37 | 12.0 | 31.6 | 0.3675 ± 0.0032 | 1.427 ± 0.017 | 1.60 ± 0.11 | 1.152 ± 0.010 | 2.63 ± 0.23 |
| D10 | Stilbite | 53.25 | 8.16 | 12.7 | 0.62 ± 0.12 | 1.426 ± 0.028 | 1.36 ± 0.27 | 1.95 ± 0.37 | 3.8 ± 0.7 |
| D11 | Stilbite | 70.12 | 9.77 | 17.1 | 0.5526 ± 0.0035 | 1.281 ± 0.039 | 1.715 ± 0.092 | 1.733 ± 0.011 | 3.81 ± 0.21 |
| D12 | Stilbite | 261.13 | 16.7 | 35.7 | 0.4534 ± 0.0061 | 1.445 ± 0.047 | 2.10 ± 0.11 | 1.422 ± 0.019 | 4.31 ± 0.24 |
| D13 | Stilbite | 47.90 | 20.9 | 44.7 | 0.454 ± 0.036 | 1.125 ± 0.038 | — | 1.42 ± 0.11 | — |
| D14 | Stilbite | 214.01 | 24.6 | 42.7 | 0.557 ± 0.028 | 1.294 ± 0.037 | — | 1.748 ± 0.087 | — |

[a] Zeolite, feldspar, and calcite samples were separated under the binocular. Although care was taken to avoid inclusions, the small size of some inclusions (cf. Fig. 2) may have made it impossible to avoid inclusions entirely.
[b] Ratios corrected for mass fractionation and blank contribution.

ever, only become apparent for the period of overshooting of the equilibrium conditions. In contrast, for the case of $[^{234}U]/[^{238}U]_{mineral} > [^{234}U]/[^{238}U]_{fluid}$ (rhombs in Fig. 5b), there is a retarded ingrowth of $^{230}Th$, as there is a deficit in $^{234}U$. The isochron initially rotates towards negative slopes before approaching the equiline (Fig. 5b), and the slope of the isochron underestimates the age of the system.

In a $[^{230}Th]/[^{232}Th]$-$[^{238}U]/[^{232}Th]$ activity diagram, stilbite data from both Svappavara and Malmberget specimens (data from Table 4) define linear arrays with significantly steeper slopes than the equiline (Fig. 5c and 5d). In contrast to stilbite and feldspar, Malmberget calcite plots close or on the equiline at very high $[^{238}U]/[^{232}Th]$ (Fig. 5d). The alignment of the stilbite data from both occurrences is not compatible with the basic requirement of an isochron, i.e., initial $[^{234}U] = [^{238}U]$ (Fig. 5a). Instead, the data suggest that mobilization of Th and U was associated with isotopic fractionation between $^{230}Th$ and $^{232}Th$ and between $^{234}U$ and $^{238}U$ (Fig. 5b). There are two principal explanations for the observed data pattern: (i) U-gain relative to Th with $[^{234}U]/[^{238}U] \gg 1$ and (ii) two-component mixing between a closed component and an open component that is characterized by young U-loss and a high $[^{238}U]/[^{232}Th]$ (Fig. 5c). The addition of Th (including $^{230}Th$) would result in excess scatter in the $[^{230}Th]/[^{232}Th]$-$[^{238}U]/[^{232}Th]$ diagram (cf. Fig. 5c). This possibility is not further discussed as the overall mobility of Th in aqueous low-temperature fluids is low and, thus, the availability of Th is likely to be extremely low with respect to U.

The linear relationships of the stilbite data in the activity diagrams allow estimation of the respective equipoint. Using the equipoint from the $[^{230}Th]/[^{232}Th]$-$[^{238}U]/[^{232}Th]$ diagram (Fig. 5c and 5d), stilbite from Svappavara and Malmberget yields $^{238}U/^{232}Th_{atomic}$ ratios of c. 0.38 and 3.8, respectively, prevailing *before* the system was disturbed. Although these values have large uncertainties—either from the scatter of the data (Svappavara) or the extrapolation from high $[^{238}U]/[^{232}Th]$ values (Malmberget)—they fall in the same range as the $^{238}U/^{232}Th_{atomic}$ ratios estimated from the Pb isotopes (Fig. 4). The similarity of the $^{238}U/^{232}Th_{atomic}$ estimates derived from two different isotope systems strongly argues against repeated disturbance of the Th-U systematics with significant Th-U fractionation in the distant past. Instead, the data imply a relatively "young" age for the disturbance of the Th-U-Pb systematics, i.e., distinctly less than one million years. The measured $^{238}U/^{232}Th$ values of all stilbite fractions fall to the right of the equipoint estimated from the Pb isotope systematics. For a homogeneous system, this implies an overall U-gain during the last major disturbance. For a two-component system, one open-system component having a high $^{238}U/^{232}Th$ and one closed-system component having a low $^{238}U/^{232}Th$ value, this data pattern indicates that most of the Th is bound in the closed-system component, allowing the $^{238}U/^{232}Th$ of the open system to become very high (cf. Fig. 5d). If the open-system end member was in activity equilibrium before disturbance, the data align along a linear trend. An end member in activity disequilibrium before disturbance eventually results in a scattered mixing trend, as could be the case in Figure 5c. The similarity of the equipoints derived from the Th-U and Pb-Pb systematics suggests that the radiogenic Pb is bound to the closed system rather than to the open system. This is also indicated by the results of the leaching experiments (Table 1). Thus, the Th/U as derived from the Pb isotope systematics does not necessarily reflect a value representative for the entire sample, but rather the value of the less mobile components in the sample. If Pb is lost from the channel sites to the silicate framework, one would not only obtain similar Th/U estimates from both approaches, but also a marked excess in radiogenic Pb. A possible transfer mechanism is presented in section 6.3. Since Th/U derived from the Pb systematics and the Th-U-disequilibrium system integrate over entirely different time scales, apparent bulk U-loss for one system and apparent U-gain for the other one do not necessarily have to be in conflict with each other.

#### 6.1.1. U-gain relative to Th with $[^{234}U]/[^{238}U] \gg 1$

Surface and groundwaters, as well as hydrothermal fluids, are generally characterized by activity disequilibrium between $^{234}U$ and $^{238}U$ (e.g., Osmond and Cowart, 1976; Osmond and Cowart, 1992). The $[^{234}U]/[^{238}U]$ ratio is close to 1.144 in seawater (e.g., Chen et al., 1986) and ranges typically between 1 and 2 in surface waters (Osmond and Cowart, 1992). The range of this ratio is significantly higher in groundwaters and hydrothermal fluids ($[^{234}U]/[^{238}U] = 1$–30; e.g., Osmond and Cowart, 1976; Osmond and Cowart, 1992; Frank, 1997). The relative enrichment of $^{234}U$ in fluids is generally interpreted as being due to higher leachability of $^{234}U$, whose grandparent $^{234}Th$ was displaced by α-recoil from its original lattice site (e.g., Kigoshi, 1971; Fleischer, 1980). The uptake of U from percolating fluids with high $[^{234}U]/[^{238}U]$ shifts the data to the right in a $[^{230}Th]/[^{232}Th]$-$[^{238}U]/[^{232}Th]$ diagram and eventually results in the "overshooting" of the equiline (circles in Fig. 5b). The alignment of the Malmberget data along a common line suggests that all fractions had the same postdisturbance $[^{234}U]/[^{238}U]$ values at one stage of their evolution. The contrasting slopes of the trends of stilbite from the Svappavara and Malmberget species in the $[^{230}Th]/[^{232}Th]$-$[^{238}U]/[^{232}Th]$ diagram (Fig. 5c and 5d) implies that stilbite from the two specimens had either different postdisturbance $[^{234}U]/[^{238}U]$ values or have been disturbed at different times. Note that the uptake of U from a fluid cannot be due to mining activity over the last 300 yr because of the insufficient time to allow for the required $^{230}Th$ ingrowth and the reduction of the $[^{234}U]/[^{238}U]$ excess to the present values of 1.1 to 1.6 (Table 4).

#### 6.1.2. Two-component mixing

The stilbite concentrates from Svappavara and Malmberget differ drastically in their respective U contents (Table 4). Detailed microprobe work revealed that some high-U stilbite from Malmberget contains small inclusions of K-feldspar, Fe-sulfides, calcite, apatite, and monazite (Fig. 2). In contrast, the low U stilbite from Svappavara is generally free of inclusions. Fractures and grain boundaries of stilbite from both Malmberget and Svappavara have a "dusty" appearance that is due to submicroscopical grains of Fe oxides and Fe sulfides. Although care was taken to avoid inclusions, some concentrates from Malmberget almost certainly represent mixtures between stilbite and U-Th-Pb-bearing phosphates (apatite, monazite).

The Th-U-(Pb) systematics of stilbite from Malmberget and Svappavara can be modeled as a two-component mixture of a young stilbite-bound open-system component (high $[^{238}U]/[^{232}Th]$ position in Fig. 5c) and an old closed-system component (low $[^{238}U]/[^{232}Th]$ falling on the equiline) representing the mineral inclusions. The good alignment of the stilbite data to a linear trend in the $[^{230}Th]/[^{232}Th]$-$[^{238}U]/[^{232}Th]$ diagram (Fig. 5c) requires that the open-system end member was isotopically well-defined. This means that this end member should have been close to activity equilibrium, i.e., any previous disturbance of this end member was old in terms of Th-U-disequilibrum dating. Otherwise there would be significant scatter. For a recent disturbance, the open system part is moved to the left of the equiline for U-loss (Fig. 5c). Together, the two systems define a mixing line with a steeper slope than the equiline. With time, the line has been rotated back to a flatter slope. Since the initial position of the assumed mixing line is not known, the present slope of the mixing line can not be used to estimate the age of the disturbance. The two-component mixing scenario illustrated in Figure 5c indicates that Th/U in the closed-system end member is significantly higher than in the open-system end member, suggesting that Th is dominantly hosted in inclusions such as apatite and monazite. The open-system end member would then be represented by channel-bound U and surface-adsorbed U. This interpretation agrees well with the observed $^{238}U/^{232}Th_{atomic}$ values from the leaching experiment. The values range from 222 and 250 in early leach steps to 125 in intermediate steps and 18 in the residue (calculated from data in Table 1). This indicates that most of the U is hosted in the easily exchangeable channel sites and that some U and Th may in fact reside in monazite inclusions such as those observed in BSE images (Fig. 2). A minimum predisturbance $^{238}U/^{232}Th$ ratio can be estimated for the open-system end member for the sample with the highest $[^{230}Th]/[^{232}Th]$ and the assumption that $[^{234}U]/[^{238}U] > 1$. Using the respective minimum predisturbance $^{238}U/^{232}Th$ value for stilbite from the Svappavara and Malmberget specimen suites and the intercept of the equilines with the respective regression lines, we conclude that the bulk of U in either sample suite is contained in the easily exchanged channel sites. This conclusion is important for the following discussion.

### 6.2. $^{234}U/^{238}U$ vs. $^{230}Th/^{238}U$ Systematics

The stilbite data of both localities scatter widely in a $[^{234}U]/[^{238}U]$-$[^{230}Th]/[^{238}U]$ diagram (Fig. 6a and 6b). This diagram illustrates the temporal evolution of activity ratios within the $^{238}U$ decay series for initial $[^{234}U]/[^{238}U]$ disequilibrium. The grid shows the temporal isotope evolution in an initially $^{230}Th$-free system, as would be typical for minerals precipitated from an aqueous solution. As the disturbance of the system did not remove significant amounts of $^{230}Th$ from stilbite, the age values shown in the grid are necessarily too old. The scatter of the data implies that individual stilbite fractions have had a wide range of initial $[^{234}U]/[^{238}U]$ values that were larger than unity (Fig. 6). Such enhanced $[^{234}U]/[^{238}U]$ values can be explained either by: (i) uptake of U from a fluid that is characterized by excess $^{234}U$, a common feature of groundwater, (ii) implantation of $^{234}Th$ into the crystal lattice through α-recoil, and (iii) preferential loss of the long-living isotopes $^{238}U$ and $^{235}U$ relative to $^{234}U$. The data pattern of stilbite and alkalifeldspar from the Malmberget specimen can be explained by any of these three processes. Both the uptake of U from a fluid and the implantation of $^{234}Th$ (grandparent of $^{234}U$) by α-recoil would require at least 50 to 100 ka—depending on the starting isotope composition—to develop the observed $[^{230}Th]/[^{238}U] > 1$ (Fig. 6b). In contrast, preferential loss of $^{238}U$ and $^{235}U$ shifts the data to both higher $[^{234}U]/[^{238}U]$ and $[^{230}Th]/[^{238}U]$ values and allows little constraints regarding the time of disturbance (Fig. 6b). The lower the $[^{234}U]/[^{238}U]$ of the lost U, the younger the age calculated for the U loss. The pattern of Svappavara stilbite can not be explained by a single stage of U-uptake or bulk U-loss (Fig. 6a). Instead, the Svappavara concentrates suggest a preferential loss of the long-lived U isotope $^{238}U$ relative to $^{234}U$ or a multistage evolution.

The preferential mobilization of $^{238}U$ (and $^{235}U$) relative to

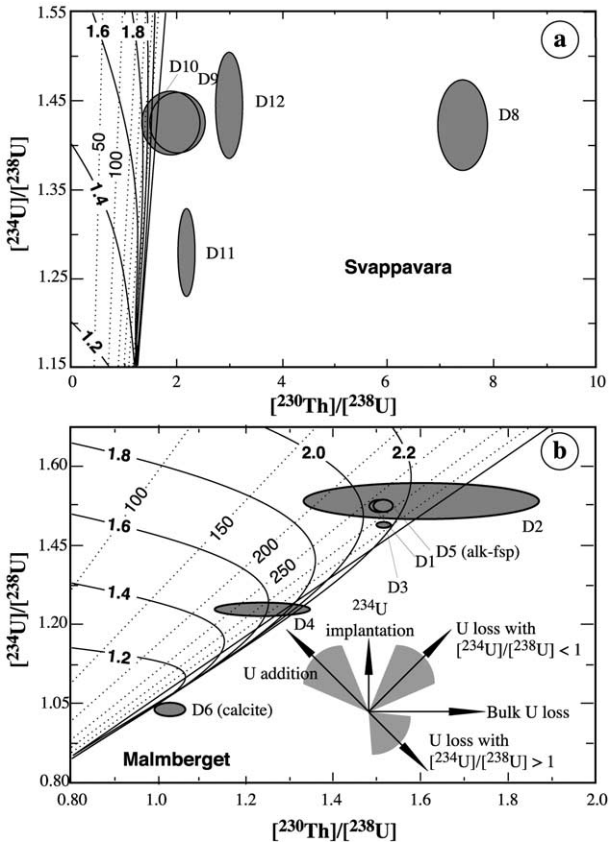


Fig. 6. $[^{234}U]/[^{238}U]$-$[^{230}Th]/[^{238}U]$ diagram for stilbite concentrates from Svappavara and Malmberget, respectively. Fraction numbers as in Table 4. Arrows indicate schematically how the fractions would be disturbed by U mobility.

$^{234}U$ is demonstrated by the leaching experiments (Table 1). While no isotopic fractionation between $^{235}U$ and $^{238}U$ occurred, the $[^{234}U]/[^{238}U]$ ratio of U released during the leaching procedure is heterogeneous. $[^{234}U]/[^{238}U]$ values range from ~1.91 and 1.85 to 1.47 (step releasing most of the U) for leachable channel-hosted U. The $[^{234}U]/[^{238}U]$ value of the residue is 2.55 (Table 1). Thus, a strong $^{234}U$ excess in the bulk sample after the last disturbance is conspicuous. Since *in situ* growth of $^{234}U$ is not able to generate $[^{234}U]/[^{238}U]$ activity ratios larger than unity, the anomalous $^{234}U$ activity must be due to either (1) U addition from an external fluid that is characterized by a high $[^{234}U]/[^{238}U]$, or (2) preferential loss of $^{238}U$ relative to $^{234}U$. The contrasting $[^{238}U]/[^{234}U]$ values between leachates and residue clearly demonstrate that isotopic fractionation during U-loss can occur during fluid-stilbite interaction.

### 6.3. $^{230}Th/^{234}U$ vs. $^{234}U/^{238}U$ Systematics

Figure 7a schematically shows the temporal evolution of the $^{238}U$-$^{234}U$-$^{230}Th$ systematics for a system with initial activity-disequilibrium in $[^{234}U]/[^{238}U]$ and $[^{230}Th]/[^{234}U]$. From its starting point at $t_0$, each sample moves with time along a uniquely defined trajectory toward the equipoint. Note that the two extreme cases (1) $[^{234}U]/[^{238}U]_{init} = 1$ with $[^{230}Th]/[^{234}U]_{init}$ = variable, and (2) the envelope for $[^{230}Th]/[^{234}U]_{init} = 0$ and variable $[^{234}U]/[^{238}U]_{init}$, divide the diagram into four fields (sectors I, II, III, IV in Fig. 7a). The envelope (Line 2, Fig. 7b) corresponds to the extreme value of $[^{230}Th]/[^{234}U]$ that can be reached with these starting conditions. Time-trajectories originating in any of these fields do not intercept Line 1 and asymptotically approach Line 2. These two lines represent special cases: (1) Data which have $[^{234}U]/[^{238}U] = 1$ (Line 1, Fig. 7b) fulfill the requirements for an isochron and can be treated adequately in the diagram shown in Figure 5a.; (2) Data with $[^{230}Th]/[^{234}U]_{init} = 0$ fulfill the requirements to be treated in the $[^{230}Th]/[^{238}U]$ vs. $[^{234}U]/[^{238}U]$ and the $[^{230}Th]/[^{234}U]$ vs. time diagrams (Fig. 7c).

Stilbite concentrates from the Malmberget and Svappavara hand specimens show $[^{234}U]/[^{238}U]$ disequilibrium ranging from 1.2 to 1.5 and 1.1 to 1.6, respectively (Table 4, Fig. 7). The more variable $^{230}Th$ excess in the Svappavara concentrates indicates a distinct postdisturbance heterogeneity in $[^{230}Th]/[^{234}U]$ values on the hand-specimen scale. The Svappavara stilbite fractions plot into field II in Figure 7, indicating U-loss relative to Th. Thus, the $[^{234}U]/[^{238}U]$ activity disequilibrium of the Svappavara stilbite is dominantly due to the preferential loss of $^{238}U$ relative to $^{234}U$. In contrast to Svappavara stilbite, Malmberget stilbite is in or near $[^{230}Th]/[^{234}U]$ equilibrium. This implies that (1) this ratio was not disturbed and Th and U were mobilized not at all or to the same extent, or (2) the disturbance is old enough to permit reestablishing of equilibrium. This case is illustrated in Figure 7c. For an initial $[^{230}Th]/[^{234}U]$ value close to 1 (shaded band M), the age of the disturbance is poorly constrained and may take any value between the present and c. 100 ka. For an initial disequilibrium in $[^{230}Th]/[^{234}U]$, the age of the disturbance may have been increasingly older, mainly depending on the initial deviation of $[^{230}Th]/[^{234}U]$ from equilibrium and to a lesser extent on the initial $[^{234}U]/[^{238}U]$ (Fig. 7c).

Addition of U lowers the $[^{230}Th]/[^{234}U]$ of the sample. Since Th is distinctly less soluble in surface and low-temperature waters than U (Allard et al., 1984; Kaplan et al., 1994), it is unlikely that the addition of U is balanced by the addition of Th. U-addition should reduce the $[^{230}Th]/[^{234}U]$ ratio to values distinctly less than unity for samples that had been in activity equilibrium. The addition of U with $[^{234}U]/[^{238}U] > 1$ will shift the data into field IV in Figures 7a and 7b. Only stilbite from Malmberget falls into this field IV (Fig. 7a) and, thus, their Th and U isotope systematics can be also explained by the addition of U in the past.

Stilbite from Malmberget and Svappavara has $[^{234}U]/[^{238}U]$ ratios distinctly >1. Because the addition of "anomalous" U with high $[^{234}U]/[^{238}U]$ is not feasible to explain the position of Svappavara stilbite in a $[^{230}Th]/[^{234}U]$-$[^{234}U]/[^{238}U]$ diagram (Fig. 7), fractionation of U isotopes during U-loss must be an important process. In all fractions, the measured $^{238}U/^{235}U_{atomic}$ was, within analytical uncertainties, identical to the natural value of 137.88. This implies that both long-living radioactive U isotopes behaved similarly during mobilization of U. In contrast, $^{234}U$, the intermediate daughter of the $^{238}U$-decay series, behaved differently and was fractionated against $^{238}U$ and $^{235}U$ during the mobilization processes. This strongly suggests that $\alpha$-recoil is the responsible process. We suggest implantation of $^{234}Th$ (which decays via $\beta$ decays to $^{234}Pa$ and $^{234}U$) into the stilbite silicate framework by $\alpha$-recoil. This

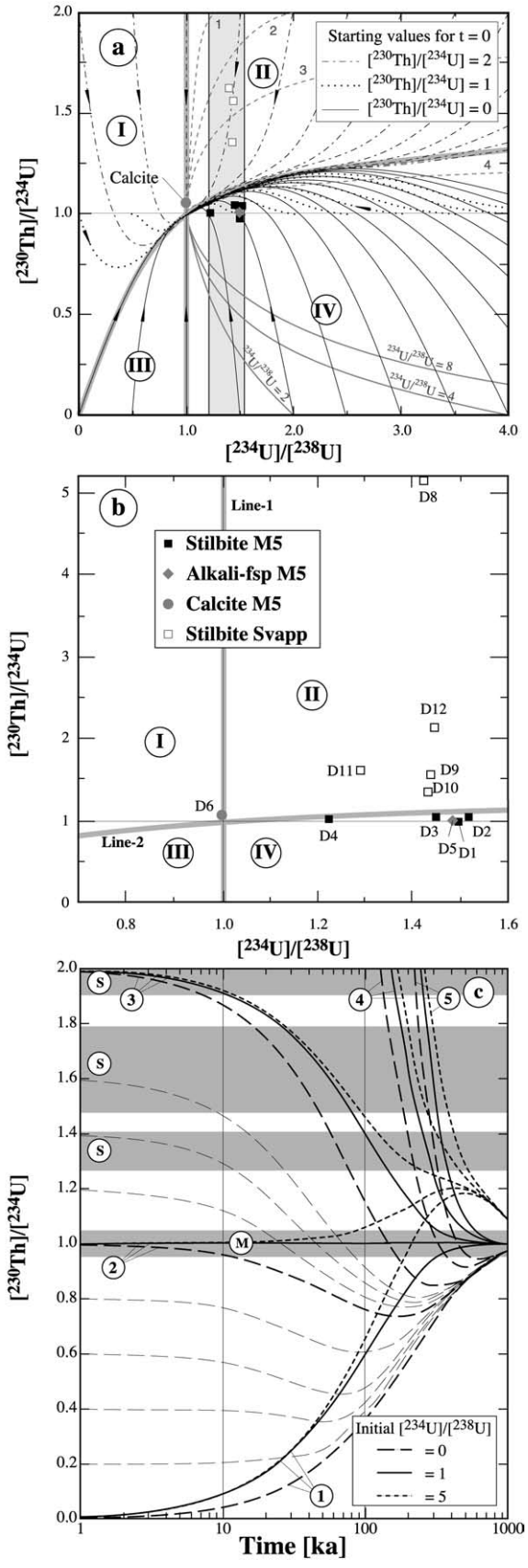


process will discriminate the leaching behavior of the recoiled daughter isotopes relative to that of the parent isotopes $^{235}U$ and $^{238}U$. This model rests on the fact that due to the recoil effect each daughter isotope in the decay series of $^{238}U$, $^{235}U$, and $^{232}Th$ is displaced from the site initially occupied by one of these long-lived parent isotopes. A good part of the $^{234}U$ resides in a different site than $^{238}U$.

### 6.4. Effects of $\alpha$-Recoil

The $\alpha$-recoil process displaces the daughter nuclei in the U decay-series by ~200 to 350 Å (e.g., Nasdala et al., 2001). In addition, it triggers off a collision cascade that creates a small structurally damaged volume. The daughter isotope, therefore, may be prone to preferential leaching, provided low-temperature processes did not anneal its travel path. Recoiled daughter isotopes of near surface U (incorporated in the crystal lattice or adsorbed on the crystal surface), $^{234}Th$ and $^{230}Th$, may be ejected from the crystal into the open fracture and thereby become lost. Such a sample would acquire a deficit in $^{234}U$ and $^{230}Th$. Loss through $\alpha$-recoil alone results in $[^{234}U]/[^{238}U]$ and $[^{230}Th]/[^{234}U]$ values $<1$. Direct loss of U-daughters by $\alpha$-recoil applies only to a less than 0.03 $\mu$m wide veneer of the crystal, and thus, is not very efficient to generate disequilibrium. Leaching of the recoiled daughter isotopes from their disturbed location in the crystal or along recoil tracks may enhance the overall loss, but does not enlarge significantly the volume from which the loss occurs. Since the solubility of Th in aqueous fluids is much lower than that of U, such kind of leaching would result in lower $[^{234}U]/[^{238}U]$ and enhanced $[^{230}Th]/[^{234}U]$ ratios in the mineral. On the other hand, recoil implantation of U daughters through mineral surfaces into inclusions, fractures, voids, and channels eventually results in excess $^{234}U$ and $^{230}Th$. Even here, only the outermost veneer of the crystal may experience a gain of U daughters. Thus, the critical parameter, which controls (i) whether an analytically resolvable excess of U daughters is obtained or not, and (ii) which magnitude such an excess may reach, is the surface-to-volume ratio. The higher this ratio, the higher the excess may become.

Fig. 7. (a) Temporal evolution of the U-disequilibrium. The four fields have the following meaning in terms of gain of Th and U (for overall loss, the $>$ and $<$ signs have to be exchanged): (I) gain $^{230}Th$ $<^{234}U$ and gain $^{234}U$ $<^{238}U$, (II) gain $^{230}Th$ $<^{234}U$ and gain $^{234}U$ $>^{238}U$, (III) gain $^{230}Th$ $>^{234}U$ and gain $^{234}U$ $<^{238}U$, and (IV) gain $^{230}Th$ $>^{234}U$ and gain $^{234}U$ $>^{238}U$. U-addition (full lines) and U-loss (dashed lines) are modeled to illustrate how the range of individual starting conditions can be reached. The $[^{234}U]/[^{238}U]$ values for U-addition are indicated in the figure, the corresponding values for U-loss are: (1) $[^{234}U]/[^{238}U] = 0.8$, (2) $[^{234}U]/[^{238}U] = 0.66$, (3) $[^{234}U]/[^{238}U] = 0.5$, (4) $[^{234}U]/[^{238}U] = 0.25$; (b) Enlargement of Figure 7A (shaded) showing the present composition of stilbite that indicates highly contrasting starting conditions for material from the two locations and among material from the same location; (c) $[^{230}Th]/[^{234}U]$-time diagram to illustrate the important effect of a $^{234}U$-deficit on the apparent age. There are five sets of curves with contrasting initial $[^{230}Th]/[^{234}U]$ values: 1: $[^{230}Th]/[^{234}U] = 0$; 2: $[^{230}Th]/[^{234}U] = 1$; 3: $[^{230}Th]/[^{234}U] = 2$; 4: $[^{230}Th]/[^{234}U] = 5$; 5: $[^{230}Th]/[^{234}U] = 10$. Grey bands correspond to the measured $[^{230}Th]/[^{234}U]$ values of stilbite concentrates from Svappavara (S) and Malmberget (M).

The surface-to-volume ratio is, for most minerals, directly related to the size of the crystals. For molecular sieves such as zeolite minerals, however, this ratio is a crystal property that is hardly related to the actual size of the crystal. The investigated calcite has a small surface-to-volume ratio. Therefore, it will essentially not obtain any activity disequilibrium. The altered alkalifeldspar has a large surface-to-volume ratio. It had been strongly altered by the hydrothermal fluids that deposited stilbite and calcite. Furthermore, it is highly fractured and contains abundant small inclusions of U-rich calcite. Therefore, recoil implantation is more important in this alkalifeldspar. The surface-to-volume ratio is exorbitantly high for stilbite, which has an open framework structure with intersecting 8-member and 10-member rings of linked $SiO_4^{4-}$ tetrahedra. The channels have diameters of 2.7 × 5.6 Å and 4.9 × 6.1 Å (e.g., Szostack, 1992). Thus, an $\alpha$-recoiled daughter isotope may have intersected more than 10 channels, damaging the channel walls. Low-temperature annealing of these channel walls may render the recoiled daughter isotope eventually unavailable for the same mobilization processes that act upon ions hosted in the channels and along fractures. Recoil displacement of U-daughters in a fine-grained carbonate-silicate mixture has been shown to affect the $^{230}Th/^{238}U$ age of the carbonate fraction (Henderson et al., 2001). While this effect is only small in the fine-grained carbonate-silicate mixture, the extreme surface-to-volume ratio of zeolite minerals could allow this effect to become very important in stilbite.

Channel-hosted U is highly mobile in stilbite as demonstrated by the leaching experiments (Sections 4.2 and 4.3). The contrasting behavior of $^{238}U$ and $^{235}U$ from $^{234}U$ may indicate a higher mobility of the channel-hosted $^{238}U$ and $^{235}U$ relative to $^{234}U$ displaced from its original channel site by $\alpha$-recoil of $^{234}Th$. We suggest that this contrasting isotope mobility due to $\alpha$-recoil may explain the variability of the Svappavara data in the $[^{230}Th]/[^{234}U]$-$[^{234}U]/[^{238}U]$ diagram (Fig. 7). As demonstrated above, all stilbite fractions from Svappavara are compatible with variable U-loss as indicated by $[^{230}Th]/[^{234}U] > 1$ and $[^{234}U]/[^{238}U] > 1$ (Fig. 7b and 7c). Such a process is also possible for the Malmberget stilbite, but does not necessarily represent the only interpretation for this specimen. Alternatively, the Malmberget data can be explained by (i) a polystage system with significant (>90%) U loss followed by U gain with $[^{234}U]/[^{238}U] > 1$ or (ii) uptake of radiogenic Pb paralleled by U gain with $[^{234}U]/[^{238}U] > 1$.

The leaching experiments (Table 1) demonstrate a marked $Pb_{rad}$ excess relative to U. The Pb excess is strongest for late leachates and the residue, the latter showing the most radiogenic Pb. Values for $^{206}Pb_{rad}/^{238}U$ in these leachates were >3 (calculated from Table 1), whereas a value of 0.308 would correspond to a 1.73 Ga old closed system. Such a large contrast can hardly be reconciled with the presence of distinct mineral inclusions, but may rather indicate $\alpha$-recoil implantation of U daughters into the silicate framework and their subsequent fixing by continuous low-temperature annealing of the damaged crystal lattice. In such a scenario, the suggested two-component system would consist of a subsystem hosted in the silicate framework and another one hosted in the channels. As long as actual inclusions of distinct mineral phases are subordinate, such a two-component system can explain all observations by U loss, whereby the lost component would have a deficit in $^{234}U$. Since most of the U is hosted in the easily exchangeable channel sites, while the mobility of most recoiled daughter isotopes may have been reduced according to the model outlined above, such a U loss is able to explain: (i) the excess of $Pb_{rad}$, (ii) the coincidence of $Th/U_{at}$ as determined from the $^{208}Pb_{rad}/^{206}Pb_{rad}$ and Th-U disequilibrium systematics, (iii) the steep slope in the $[^{230}Th]/[^{232}Th]$-$[^{238}U]/[^{232}Th]$ diagram, and (iv) the $[^{234}U]/[^{238}U]$ and $[^{230}Th]/[^{238}U]$ ratios >1. It is, however, not possible to deduce an exact age for this disturbance, but it is clear that it must have occurred less than one Ma ago. It should also be remembered that, because of the general open-system behavior of stilbite, $\alpha$-recoil is an attractive, although not the only possible, explanation. For instance, the plot of all diseqilibrium data to the right of the equipoint (Fig. 5) as derived from the Pb-isotopes (Fig. 4) requires that there also had been phases of U addition.

## 7. CONCLUSIONS

Stilbite from Malmberget and Svappavara is characterized by excess in $Pb_{rad}$ relative to U, $[^{234}U]/[^{238}U] > 1$, and $[^{230}Th]/[^{238}U] > 1$. Activity disequilibrium requires a disturbance of the U-Th systematics within the last one million years. The Th-U disequilibrium systematics can be explained by two different processes: (1) By addition of U with $[^{234}U]/[^{238}U] > 1$ from a fluid. This process can explain the $^{238}U$-$^{234}U$-$^{230}Th$ systematics of Malmberget stilbite. To explain its U-Pb systematics, an earlier U loss or, alternatively, addition of radiogenic Pb is necessary. In contrast, the $^{238}U$-$^{234}U$-$^{230}Th$ systematics of Svappavara stilbite require a more excessive and variable U loss (after the initial addition of U); (2) The $^{238}U$-$^{234}U$-$^{230}Th$ systematics of both systems reflects two-component mixing of elements derived from a closed and an open, channel-bound system. The open system is characterized by low $Th/U_{atomic}$ ratios. The closed system has $Th/U_{atomic}$ ratios similar to those calculated from the $^{208}Pb_{rad}/^{206}Pb_{rad}$ of stilbite fractions from both localities. It may be represented by both the silicate framework of stilbite and the small phosphate inclusions. This model suggests nearly identical mobilization histories for stilbite from Malmberget and Svappavara, in spite of significant different concentrations of Th and U. U-loss from the channels explains the linear trends in the $[^{238}U]/[^{232}Th]$-$[^{230}Th]/[^{232}Th]$ diagram (Fig. 5), as well as the position of the Svappavara fractions in the $[^{234}U]/[^{238}U]$-$[^{230}Th]/[^{238}U]$ diagram (Fig. 6). In addition, it is also compatible with the position of the Malmberget fractions in the latter diagram. U-loss from the channels also requires that $^{238}U$ (and $^{235}U$) are preferentially lost relative to the recoiled daughter isotopes (e.g., $^{234}U$, $^{230}Th$, and $Pb_{rad}$) to explain the U-Pb-Th systematics (Fig. 4). Since each $\alpha$-recoil displaces the daughter isotope by a distance of more than 10 unite cells within the stilbite lattice, each recoil cascade damages the silicate framework and provides a possibility that the recoiled daughter isotopes become immobile during subsequent low-temperature annealing. The combination of U loss with reduced mobility of recoil-displaced daughter isotopes can account for: (i) the Th-U disequilibrium systematics, (ii) the similarity of $Th/U_{atomic}$ as determined from the Th-U disequilibrium data and from the Pb isotope data, and (iii) the $Pb_{rad}$ excess. The closed system in this mixing model includes such recoiled isotopes and does not necessarily repre-

sent a separate mineral phase. Since the "distribution" of the open and closed system occurs at the nanometer scale, the $[^{234}U]/[^{238}U]$ excess represents a material property that is independent of the U-content and reflects the annealing efficiency and the likelihood that recoiled daughter isotopes can be immobilized. This interpretation would also explain the narrow range of $[^{234}U]/[^{238}U]$ values (1.6–1.45) in stilbite observed at both locations, with lower values (1.1–1.3) possibly originating from closed-system mineral inclusions having equilibrium values of ~1.

The two suggested models involve multistage or multicomponent systems, respectively. Therefore, they do not provide any age constraints beyond a disturbance of the U-Th systematics within the last one million years. Although the isotope data from bulk analyses do not favor either explanation, the results of our leaching experiments are more plausibly to reconcile with the mixing model. These experiments demonstrate that early released U and Pb is characterized by lower $[^{234}U]/[^{238}U]$ and $^{206}Pb/^{204}Pb$, respectively, as compared to later leaches and the residues.

*Acknowledgment*—Analytical work was done at GeoForschungsZentrum Potsdam. The analyzed specimen from Svappavara was donated by Jan-Anders Perdahl and Olof Martinsson (Luleå). Specimen M5 was donated by Aksel Österlöf (Luleå). We gratefully acknowledge Bernd Kober (Heidelberg) and Tony Eisenhauer (Kiel) for kindly providing gravimetric Th and U solutions and Hu-1 Standard solution, respectively. We thank Mrs. Cathrin Schulz for skilled help in the laboratory. We gratefully acknowledge the constructive reviews by two anonymous reviewers and L. Neymark.

*Associate editor:* Y. Amelin

## REFERENCES

Allard B., Olofsson U., and Torstenfeldt B. (1984) Environmental actinide chemistry. *Inorg. Chim. Acta* **94,** 205–221.

Allègre C. J. and Condomines M. (1976) Fine chronology of volcanic processes using 238U-230Th systematics. *Earth Planet. Sci. Lett.* **28,** 395–406.

Bernat M. and Goldberg E. D. (1969) Thorium isotopes in the marine environment. *Earth Planet Sci. Lett.* **5,** 308–312.

Breck D. W. (1973) *Zeolite molecular sieves.* Wiley.

Chen J. H., Edwards R. L., and Wasserburg G. J. (1986) *238U,* $^{234}U$, and $^{232}Th$ in sea water. *Earth Planet. Sci. Lett.* **80,** 241–251.

Chipera S. J. and Apps J. S. (2001). Geochemical stability of natural zeolites. In *Natural Zeolites: Occurrence, Properties, Applications* (ed. D. L. Bish and D. W. Ming) *Rev. Mineral. Geochem.* **45,** 117–161.

Denton G. H. and Hughes T. J. (1981) *The Last Great Ice Sheets.* Wiley.

Edwards R. L., Chen J. H., and Wasserburg G. J. (1986) $^{238}U$-$^{234}U$-$^{230}Th$-$^{232}Th$ systematics and the precise measurement of time over the past 500,000 years. *Earth Planet. Sci. Lett.* **81,** 175–192.

Faure G. (1986) *Principles of Isotope Geology* (2nd ed.). Wiley.

Flanigan E. M. and Mumpton F. A. (1981) Commercial properties of natural zeolites. In *Mineralogy and Geology of Natural Zeolites* (ed. F.A. Mumpton), *Reviews in Mineralogy* **4**, 165–175.

Fleischer R. L. (1980) Isotopic disequilibrium of uranium alpha-recoil damage and preferential solution effect. *Science* **207,** 979–981.

Flink G. (1924) *Bidrag till Malmbergsgruvornas och Kiirunavaaras mineralogi* (Contribution to the mineralogy of the Malmberget mines and Kiirunavaara). Vetenskapliga och praktiska undersökningar i Lappland anordnade av Luossavaara-Kiirunavaara Aktiebolag. (in Swedish).

Frank N. (1997) Anwendung der Thermionen-Massenspektrometrie zur Uranreihen-Datierung pleistozäner, mitteleuropäischer Travertinvorkommen. Ph.D. Thesis, University Heidelberg.

Frietsch R., Tuisku P., Martinsson O., and Perdahl J.-A. (1997) Early Proterozoic Cu-(Au) and Fe ore deposits associated with regional Na-Cl metasomatism in northern Fennoscandia. *Ore Geol. Reviews* **12,** 1–34.

Gerdes A., Weisshaar R., Mengel K., and Mangini A. (1999) U/Th-Ungleichgewichte in sekundären Kluftmineralen aus Graniten des HRL Aspö und FL Grimsel. *Berichte der Deutschen Mineralogischen Gesellschaft* **1(1999),** 81.

Henderson G. M., Slowey N. C., and Fleisher M. Q. (2001) U-Th dating of carbonate platform and slope sediments. *Geochim. Cosmochim. Acta* **65,** 2757–2770.

Jaffey A. H., Flynn K. F., Glendenin L. F., Wentley W. C., and Essling A. M. (1971) Precision measurements of half-lives and specific activities of $^{235}U$ and $^{238}U$. *Phys. Rev. C* **4,** 1889–1906.

Kaplan D. L., Bertsch P. M., Adriano D. C., and Orlandini K. A. (1994) Actinide association with groundwater colloids in a coastal plain aquifer. *Radiochim. Acta* 66/67 181–187.

Kigoshi K. (1971) Alpha-recoil thorium-234: dissolution into water and the uranium-234/uranium-238 disequilibrium in nature. *Science* **173,** 47–48.

Koul S. L., Chadderton L. T., and Brooks C. K. (1981) Fission track dating of zeolites. *Nature* **294,** 347–350.

Liou J. G., deCapitani C., and Frei M. (1991) Zeolite equilibria in the System $CaAl_2Si_2O_8$-$NaAlSi_3O_8$-$SiO_2$-$H_2O$. *New Zealand J. Geol. Geophys.* **34,** 293–302.

Ludwig K. R. (1994) ISOPLOT–A plotting and regression program for radiogenic-isotope data. Version 2 **71,** USGS Open-File Rept. 91–445.

Manhès G., Minster J. F., and Allègre C. J. (1978) Comparative uranium-thorium-lead and rubidium-strontium study of the Saint Séverin amphoterite: consequences for early solar system chronology. *Earth Planet. Sci. Lett.* **39,** 14–24.

Nasdala L., Wenzel T., Wenzel M., Vavra G., Irmer G., and Kober B. (2001) Metamictisation of natural zircon: Accumulation versus thermal annealing of radioactivity-induced damage. *Contrib. Mineral. Petrol.* **141,** 125–144.

Osmond J. K., and Cowart J. B. (1976) The theory and uses of natural uranium isotopic variations in hydrology. *Atomic. Energy Rev.* **14,** 621–679.

Osmond J. K., and Cowart J. B. (1992) Groundwater. In *Uranium-series Disequilibrium: Applications to Earth, Marine, and Environmental Sciences* 2nd Edition (ed. Ivanovich M. and Harmon R. S.), pp. 290–333, Clarendon Press.

Romer R. L. (1996) U-Pb systematics of stilbite-bearing low-temperature mineral assemblages from the Malmberget iron ore, northern Sweden. *Geochim. Cosmochim. Acta* **60,** 1951–1966.

Romer R. L., and Bax G. (1992) The rhombohedral framework of the Scandinavian Caledonides and their foreland. *Geol. Rundsch.* **81,** 391–401.

Romer R. L., and Wright J. E. (1993) Lead mobilization during tectonic reactivation of the western Baltic Shield. *Geochim. Cosmochim. Acta* **57,** 2555–2570.

Romer R. L., Martinsson O., and Perdahl J.-A. (1994) Geochronology of the Kiruna iron ores and hydrothermal alterations. *Econ. Geol.* **89,** 1249–1261.

Skiöld T. (1988) Implications of new U-Pb zircon chronology to early Proterozoic crustal accretion in northern Sweden. *Precambrian Res.* **26,** 1–13.

Steiger R. H., and Jäger E. (1977) Convention on the use of decay constants in geo- and cosmochronology. *Earth Planet. Sci. Lett.* **36,** 359–362.

Sturchio N. C., Bohlke J. K., and Binz C. M. (1989) Radium-thorium disequilibrium and zeolite-water exchange in a Yellowstone hydrothermal environment. *Geochim. Cosmochim. Acta* **53,** 1025–1034.

Szostack R. (1992) *Handbook of Molecular Sieves* Van Nostrand Reinhold.

Tilton G. R. (1973) Isotopic lead ages of chondritic meteorites. *Earth Planet. Sci. Lett.* **19,** 321–329.

Townsend R. P. (1991) Ion exchange in zeolites. In *Introduction to Zeolite Science and Practice* (ed. H. van Bekkum et al.), *Studies in Surface Science and Catalysis* **58,** 359–390.